The Astrophysical Journal, 628:210–230, 2005 July 20
© 2005. The American Astronomical Society. All rights reserved. Printed in U.S.A.

THE STELLAR CONTENT OF NEARBY STAR-FORMING GALAXIES. III. UNRAVELLING THE NATURE OF THE DIFFUSE ULTRAVIOLET LIGHT[1]

Rupali Chandar,[2] Claus Leitherer,[2] Christy A. Tremonti,[3] Daniela Calzetti,[2] Alessandra Aloisi,[2,4] Gerhardt R. Meurer,[5] and Duilia de Mello[6,7]

Received 2004 December 22; accepted 2005 March 23

ABSTRACT

We investigate the nature of the diffuse intracluster ultraviolet light seen in 12 local starburst galaxies, using long-slit ultraviolet spectroscopy obtained with the Space Telescope Imaging Spectrograph (STIS) aboard the *Hubble Space Telescope* (*HST*). We take this faint intracluster light to be the field in each galaxy and compare its spectroscopic signature with Starburst99 evolutionary synthesis models and with neighboring star clusters. Our main result is that the diffuse ultraviolet light in 11 of the 12 starbursts lacks the strong O star wind features that are clearly visible in spectra of luminous clusters in the same galaxies. The difference in stellar features dominating cluster and field spectra indicates that the field light comes primarily from a different stellar population and not from scattering of UV photons originating in the massive clusters. A cut along the spatial direction of the UV spectra establishes that the field light is not smooth but rather shows numerous "bumps and wiggles." Roughly 30%–60% of these faint peaks seen in field regions of the closest (<4 Mpc) starbursts appear to be resolved, suggesting a contribution from superpositions of stars and/or faint star clusters. Complementary WFPC2 *UVI* imaging for the three nearest target galaxies, NGC 4214, NGC 4449, and NGC 5253, is used to obtain a broader picture and establish that all three galaxies have a dispersed population of unresolved, luminous blue sources. Because the field spectra are dominated by B stars, we suggest that the individual sources observed in the WFPC2 images are individual B stars (rather than O stars) or small star clusters. We consider several scenarios to understand the lack of observed massive stars in the field and their implications for the origin of the field stellar population. If the field stellar populations formed in situ, the field must have either an IMF that is steeper than Salpeter ($\alpha \sim -3.0$ to -3.5) or a Salpeter slope with an upper mass cutoff of 30–50 $M_{\odot}$. If star formation occurs primarily in star clusters, the field could be composed of older, faded clusters and/or a population that is coeval with the luminous clusters but lower in mass. We use these benchmark populations to place constraints on the field stellar population origin. Although the field probably includes stars of different ages, the UV light is dominated by the youngest stellar populations in the field. If the field is composed of older, dissolving clusters, we estimate that star clusters (regardless of mass) need to dissolve on timescales 7–10 Myr to create the field. If the field is composed of young clusters that fall below the detection limit of individual sources in our spectroscopy, they would have to be several hundred solar masses or less, in order to be deficient in O stars, despite their extreme youth.

Subject headings: galaxies: starburst — galaxies: stellar content — ultraviolet: galaxies

Online material: color figure

1. INTRODUCTION

Nearby starburst galaxies are fundamental testing grounds for key questions related to both star formation and galaxy evolution, as well as the interplay between galaxies and their surroundings. A detailed understanding of the properties of local starbursts is also critical to further examine star-forming galaxies at high redshift, since the star formation rates of these distant, young galaxies are most similar to those found in local starbursts (e.g., Steidel et al. 1996). However, we are still learning about the stellar content and properties of local UV-bright starbursts. Meurer et al. (1995) showed that nearby starbursts are irregular structures consisting of diffusely distributed light interspersed with prominent star clusters, including both compact objects (with half-light radii $\lesssim$10 pc) and more extended OB associations. They estimate that clusters only contribute $\sim$20% of the light seen in ultraviolet images of starburst galaxies (Meurer et al. 1995; Maoz et al. 1996). Thus, the diffusely distributed light actually dominates the starburst, comprising roughly 80% of the total in the UV. To account for the observed "bimodal" nature of stellar populations in starbursts, Meurer et al. (1995) suggested that two modes of star formation occur in high-intensity bursts: prominent cluster formation and dominant diffusely distributed star formation.

Several explanations besides star formation occurring in a "cluster" mode and a "field" mode can explain the observed dichotomy of stellar properties in local starbursts. Currently one popular scenario suggests that the diffuse UV field light is created via dissipation of aging star clusters, which contribute their remaining stars to the field. There are several works that indirectly support this scenario (e.g., Tremonti et al. 2001; Lada & Lada 2003; Fall et al. 2005).

[1] Based on observations with the NASA/ESA *Hubble Space Telescope*, obtained at the Space Telescope Science Institute, which is operated by the Association of Universities for Research in Astronomy, Inc., under NASA contract NAS5-26555.

[2] Space Telescope Science Institute, 3700 San Martin Drive, Baltimore, MD 21218; rupali@stsci.edu.

[3] Steward Observatory, 933 North Cherry Avenue, Tucson, AZ 85721.

[4] On assignment from the Space Telescope Division of ESA.

[5] Johns Hopkins University, 3400 North Charles Street, Baltimore, MD 21218.

[6] Laboratory for Astronomy and Solar Physics, Code 681, Goddard Space Flight Center, Greenbelt, MD 20771.

[7] Department of Physics, Catholic University of America, 620 Michigan Avenue, Washington, DC 20064.

The stellar content of nearby starburst galaxies has been studied in more detail using multiband optical Wide Field Planetary Camera 2 (WFPC2) photometry. In addition to star clusters, color-magnitude diagram (CMD) analysis of the field star population suggests two distinct overall populations. Greggio et al. (1998) and Harris et al. (2001) find evidence that the resolved, diffuse stellar populations in NGC 1569 and M83 are older than the clusters. Tremonti et al. (2001) compared UV spectroscopy of both resolved clusters and the diffuse field light in the nearby starburst NGC 5253, with stellar evolutionary models. They established that the diffuse intracluster light in NGC 5253 has a spectrum lacking the strong O star wind features that are clearly seen in a number of the cluster spectra in this galaxy. All of these observations are consistent with a scenario where the field is composed of dissolved star clusters. A possible counterexample, which supports the concept of stars forming early on in both clusters *and* the field, is the Tosi et al. (2001) study of NGC 1705. They found that in order to reproduce the CMD of point sources in this post-starburst galaxy, a 2–3 Myr *field* star population was required.

However, other scenarios can also plausibly explain the presence of diffuse UV field light in starbursts. For example, continuous star formation in galaxies could result in a population of B stars, which originally formed in clusters over the last few hundred million years and dispersed throughout the galaxy once the clusters dissolved. A second possibility is that a fraction of UV photons originating in hot stars embedded in H II regions scatter off dust grains farther out. In 30 Doradus, UIT observations suggest that scattered light is the mechanism responsible for the UV field (Cheng et al. 1992). However, in Henize 2-10, a much more distant starburst, we were able to establish that scattered light cannot be the dominant mechanism responsible for the observed UV field (Chandar et al. 2003). Barth et al. (1995) suggested a third possibility, that the diffuse light in nuclear starburst rings may be dominated by (lower mass) unresolved star clusters. A fourth possible explanation is that individual massive stars may be forming in relative isolation in the field, as suggested for the nuclear regions of M51 (Lamers et al. 2002). Finally, in our recent work on the stellar content of He 2-10, we established that both the clusters and intracluster regions show signatures of massive stars. From our detailed simulations, we suggest that the field population that formed coevally with the neighboring compact clusters ($\sim$4–5 Myr ago) may come from less spatially concentrated "scaled OB associations" (SOBAs), which are not lacking in the most massive stars, rather than faint, low-mass coeval compact star clusters.

Is He 2-10 a unique case, where we are "catching" this galaxy early during a well-coordinated burst? Do other galaxies have field stellar populations that appear older than those of neighboring clusters, such as found in NGC 5253? Here we extend our previous studies of the diffuse intracluster light in local starbursts using long-slit STIS UV spectroscopy. Ten galaxies from our *HST* program GO-9036 have high enough signal-to-noise ratio (S/N) in the field to allow us to study their stellar composition. To these, we add the published results of He 2-10 and NGC 5253 for a more complete look at the nature of diffuse UV light in starburst galaxies.

This paper is organized as follows: In § 2 we provide background information on the galaxy sample and describe the observations, basic data reduction, and definition of the field regions. In § 3 we describe reduction and basic analysis of complementary archival WFPC2 images for three of the closest target galaxies (NGC 4214, NGC 4449, and NGC 5253). In § 4 we derive the stellar content of the field by comparing with Starburst99 models, and in § 5 we take advantage of spatial information, as well as the spectra, in order to constrain the origin of the UV field light in our sample. Finally, in § 6 we summarize the main conclusions of this work.

2. THE SAMPLE, OBSERVATIONS, AND DATA REDUCTION

2.1. *Galaxy Sample*

Our *HST* program, GO-9036, was designed to obtain a homogeneous far-ultraviolet (FUV) and near-ultraviolet (NUV) spectroscopic data set of 18 nearby starburst galaxies. The target galaxies span a broad range of morphologies, chemical compositions, and luminosities. The primary targets in each galaxy were one to three luminous clusters (either compact or giant H II regions); however, the projected $25'' \times 0\farcs2$ STIS long slit also covers fainter, serendipitous objects (which could be stars or clusters) and regions of diffuse UV emission where no obvious sources are seen in available archival Faint Object Camera (FOC) and WFPC2 images. The galaxy sample, distances, and area projected in the slit are compiled in Table 1. Additional details for the galaxy sample and observations (including slit locations) are presented in the first paper in our series (R. Chandar et al. 2005a, in preparation). Analysis of the cluster content is the focus of the second paper (R. Chandar et al. 2005b, in preparation). In this investigation, we analyze the diffuse UV emission seen between clusters in 10 target galaxies. These are the galaxies where the S/N of the extracted field spectrum is sufficiently high ($\gtrsim$10) to quantify the dominant stellar population. To these we add the results of our previous work on He 2-10 (Chandar et al. 2003) and NGC 5253 (Tremonti et al. 2001), for a comprehensive study of diffuse UV emission in 12 local starburst galaxies.

2.2. *Data Reduction*

In order to combine multiple aligned exposures of the same target, we added together the flat-fielded two-dimensional images (there were no shifts between multiple galaxy spectra taken for GO-9036), updated the exposure time in the headers to reflect the total integration time, and reprocessed through the CALSTIS pipeline. This pipeline rebins the spectra and provides a global detector linearity correction, dark subtraction, flat fielding, wavelength calibration, and conversion to absolute

TABLE 1
SAMPLE GALAXY PROPERTIES

Galaxy	Adopted Distance (Mpc)	Area Projected in Slit[a] (pc)	References
He 2-10	9	1100 × 9	1
Mrk 33	22	3150 × 25	2
NGC 1741	57	6200 × 49	3
NGC 3125	11.5	1400 × 11	4
NGC 3310	13.3	2300 × 18	5
NGC 4214	2.9	350 × 3	1
NGC 4449	3.9	550 × 4	6
NGC 4670	16	1900 × 16	4
NGC 5253	3.33	400 × 2	7
NGC 5996	47	6200 × 49	4
NGC 7552	21	2500 × 20	4
Tol 1924−416	37	5000 × 40	4

[a] Based on distance given in the second column, assuming $25''$ coverage of the galaxy and given the slit width of the observations.

REFERENCES.—(1) Kobulnicky et al. 1999; (2) Davidge 1989; (3) Guseva et al. 2000; (4) Heckman et al. 1998; (5) Pastoriza et al. 1993; (6) Boeker et al. 2001; (7) Izotov & Thuan 1999.

flux units. For subsequent analysis on the field regions we utilized these fully calibrated rectified two-dimensional images reprocessed through the CALSTIS pipeline, which have a linear wavelength scale and uniform sampling in the spatial direction. Further processing steps on the extracted one-dimensional spectra included deredshifting (values taken from NED) and rebinning to the wavelength scale of the Starburst99 models (0.75 Å pixel^{-1}) utilized for comparison with the observations. We then corrected the extracted spectra for strong geocoronal emission at Lyα and O I λ1302 by assuming that an outer portion from the two-dimensional spectrum, which is typically located near the edge of the observable galaxy, represents a purely geocoronal spectrum near the Lyα and O I λ1302 features. For each galaxy, the spectrum extracted from near the end of the slit is typically at least 10 times weaker in continuum flux than the field regions and displays very weak spectral features (if they were observable at all), indicating that these are suitable for correcting geocoronal features.

2.3. *Extraction of the Field*

In order to study the stellar content of the galaxies in our sample, we first detected objects (which could be stars or clusters) from profiles taken along the slit (700 columns were collapsed along the spatial direction). Our detection procedure is analogous to those generally used for object detection in images. Objects were defined as peaks along the spatial direction that reached a level at least 5 times higher than the standard deviation (σ) plus the local background level (a second category, faint objects, which have 3–5 σ detections, are also studied in R. Chandar et al. 2005b, in preparation). This technique ensures that we are detecting real sources and not random surface brightness fluctuations. In principle, detected objects can be either stellar clusters or individual stars. However, individual stars should be considered as part of the diffuse UV population. Therefore, it is very important to assess whether our object detection algorithm is detecting individual stars, since we do not want to exclude individual O and/or B stars from our definition of the field. Based on the depth of our data and detection limits, the possibility of excluding individual massive stars is only a concern for the closest galaxies, those within $\sim$5 Mpc. Because clusters dim as they age, the total luminosities of clusters and individual O/B supergiants can overlap, making it impractical to use a simple luminosity cut to separate stars and clusters. A further complication is that the narrow slit used in this study often does not include all of the light from an object, either because the object is extended and/or because it is not centered in the slit. Thus, it is important to consider the *total* intrinsic luminosities of detected sources and not just the light falling in the slit. To address this concern, we use a combination of object luminosities (from R. Chandar et al. 2005b, in preparation) measured at 1500 Å, which are strict lower limits, and size information (from profiles along the STIS slit and sometimes available WFPC2 images) to assess whether we are indeed detecting individual luminous stars.

Here we use NGC 5253 as an example to examine the nature of detected sources, since the FUV spectrum for this galaxy is the deepest of the three closest targets. An O supergiant has an intrinsic spectral luminosity density at 1500 Å, L_{1500}, of $\sim 5 \times 10^{35}$ ergs s^{-1} Å^{-1}. This is similar to the light falling in the STIS slit for the weakest detected objects (see, e.g., objects 3 and 11 in Tremonti et al. 2001). However, the spatial profiles for these objects are clearly resolved (as are the profiles for basically all detected objects in NGC 5253 and NGC 4214 and most objects in NGC 4449), and the slit location suggests that much of the flux from object 3 in NGC 5253 has been missed. In fact, a comparison of the total L_{1500} from available F170W WFPC2 images and STIS spectroscopy (see Table 1 in Tremonti et al. 2001) shows that for the four brightest sources, the L_{1500} flux measured from imaging where all of the light from an object is accessible is higher by factors of 4–15 than the flux measured from STIS spectroscopy. Similar arguments apply for the objects detected in NGC 4214 and NGC 4449. We conclude that the detected objects in galaxies closer than 5 Mpc are not individual luminous stars, but stellar clusters or groups of stars. For more distant galaxies object fluxes are too high to come from individual stars. Therefore, we refer to detected sources in our STIS spectra as clusters. In our analysis, we make an arbitrary distinction in each galaxy between bright clusters (S/N $>$ 10) and faint clusters (typically 4 $\leq$ S/N $\leq$ 8). These are discussed further in § 5.2.2.

We defined the field regions for each galaxy in two ways: (1) regions within 3 σ of the local background and (2) the entire galaxy minus the one to three targeted luminous clusters (those used to determine the slit orientation). The spatial pixels defined as belonging to the field were then summed to give a one-dimensional field spectrum. Note that in regions where the background changes rapidly along the slit, it can be difficult to determine the appropriate local level. To address this issue and any lingering concerns that our first definition eliminates small groups of individual O or B stars from the extracted field, we analyzed both extracted field spectra for each galaxy. We minimized contamination from luminous clusters by avoiding light from the wings of their profiles. Spatial profiles, along with field regions according to our first definition, are presented in Figure 1.

Note that a number of galaxies, particularly those with a large number of clusters in the slit (e.g., NGC 3310 and NGC 4449), also have many "bumps and wiggles" in their field portions (those within 3 σ of the local background). In fact, in most galaxies, particularly those that are nearby, star clusters are not embedded in a smooth background of UV light. The field always shows some structure. Is this structure due to variable reddening or discrete stellar populations? In § 5.4 we discuss the results of measuring the spatial extent or size of numerous faint "peaks" visible in starburst field regions through our slits. We find in general that a significant fraction of these peaks are unresolved, and those that are resolved have sizes that are comparable to luminous clusters observed in each galaxy. Additionally, we were able to match a few of the brighter peaks observed in the STIS field regions with discrete, faint sources in deeper archival WFPC2 images. Taken together, these points suggest that at least some of the faint peaks seen along the spatial direction are actually discrete stellar populations (possibly a few stars or faint compact clusters), rather than variations in extinction or random fluctuations in the background level.

2.4. *Selection Effects/Biases*

We note that the precise locations defined as the "field" in each galaxy depend on a number of factors, such as total exposure time, galaxy distance, and local background levels. Thus, the "field" as we have defined it is subject to a number of selection effects/biases. For example, deeper observations might allow for additional small bumps and wiggles in the spectrum to be added to the "object" list, as their S/N is increased. However, because we have collapsed a large number of pixels along the spatial direction, our definitions are somewhat robust against the depth of the observations. Our definition of "field" is also distance dependent in the sense that we are unable to uniformly

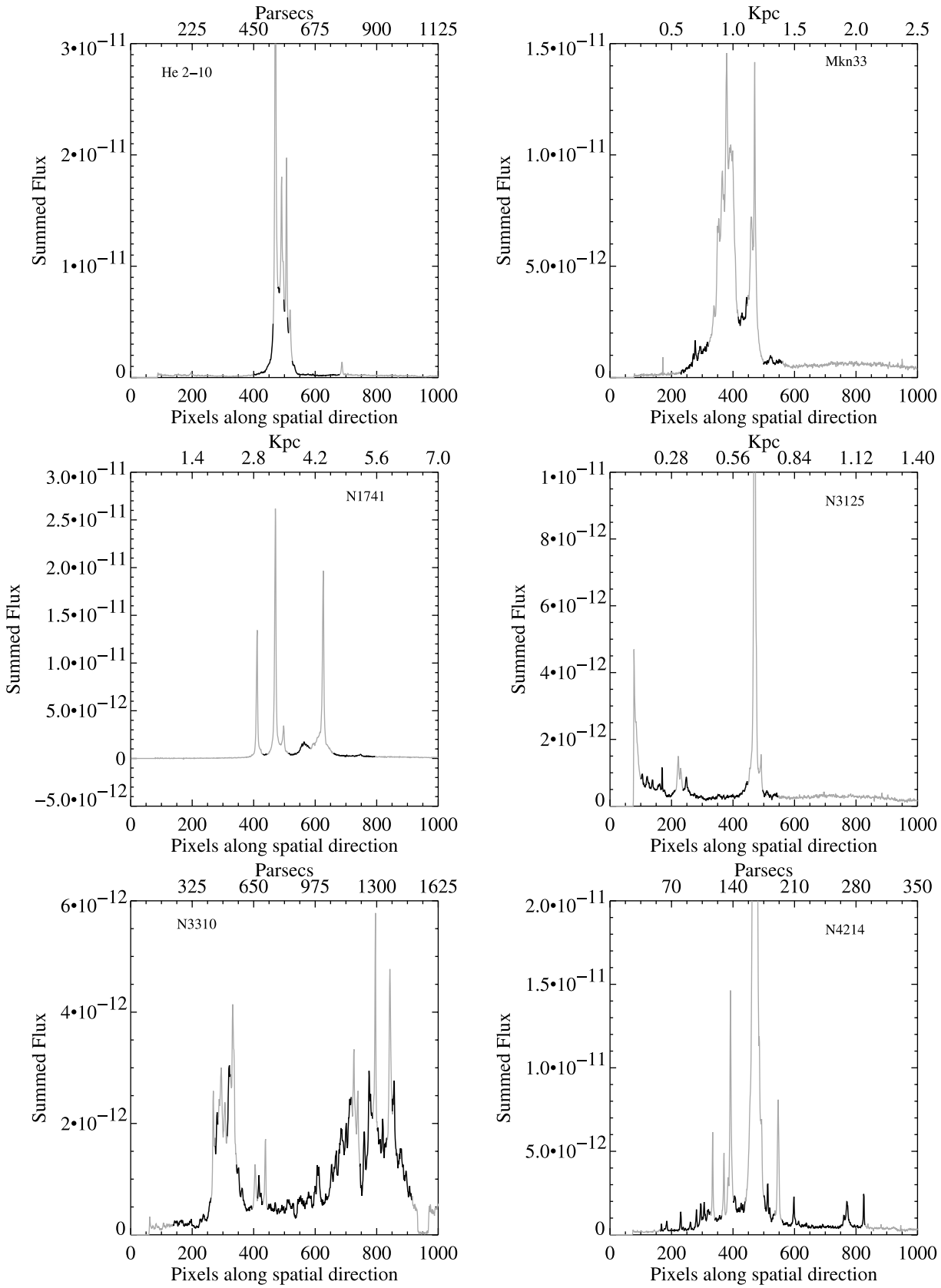


FIG. 1.—Integrated flux (from 700 pixels, ∼1250–1700 Å) as a function of position along the slit for each target galaxy in this study. The portions of the spectra that were used to create the composite field spectra are plotted in black. The STIS MAMA detectors have a plate scale of 0.″024 pixel^{-1}.

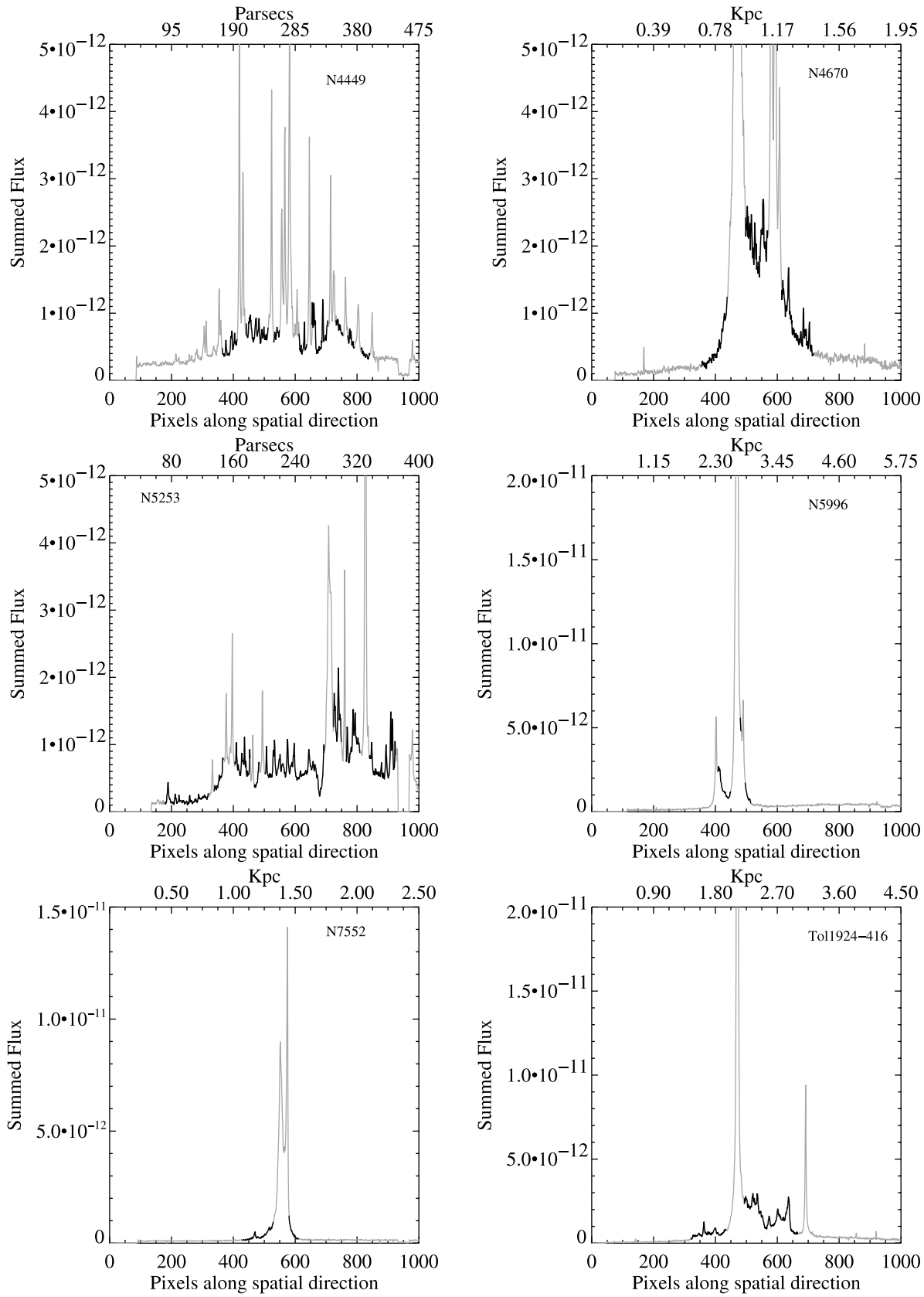


FIG. 1.—*Continued*

TABLE 2
FRACTION OF FUV LIGHT FROM CLUSTERS AND THE FIELD

Galaxy	Clusters	Field
He 2-10	0.64	0.36
Mrk 33	0.41	0.59
NGC 1741	0.54	0.46
NGC 3125	0.76	0.24
NGC 3310	0.28	0.72
NGC 4214	0.77	0.23
NGC 4449	0.38	0.62
NGC 4670	0.68	0.32
NGC 5253	0.32	0.68
NGC 5996	0.59	0.41
NGC 7552	0.57	0.43
Tol 1924−416	0.58	0.42

NOTES.—Values determined by summing up the light from spatial plots for all clusters and comparing with the total light in the slit. The spatial plots are summed over 700 pixels, covering ∼1250–1700 Å. Because the slit locations were chosen to maximize the number of UV-luminous clusters aligned in the slit, these fractions represent *lower limits* to the total fraction of field light in each galaxy.

define a minimum object mass at a given age that is selected as a cluster. More distant galaxies are more likely to have higher mass clusters hiding in the field. If some of these clusters are very young, then we would expect the signature of massive stars in the extracted field spectra to increase with galaxy distance. Potentially, some of the less massive objects that we have defined as clusters (this only applies to galaxies closer than ∼5 Mpc) may be random superpositions of several field O stars or possibly SOBAs (Hunter 1999).

Our second extraction of the field, where we have only excised targeted clusters, allows us to directly probe this issue. In § 4.1 we present results comparing the stellar content in the field and cluster spectra with instantaneous burst Starburst99 models. Although these models are not a good physical representation of the field, they do provide a simple way to quantify the massive star content. We found virtually no difference in the best-fit ages, and hence in the massive star content, in our two definitions of the field for each galaxy.

2.5. *Spatial Profiles along the Slit*

Figure 1 shows the integrated 1250–1700 Å flux along the spatial direction of our long-slit spectra. In addition to allowing us to define clusters/field portions, these spatial profiles give some insight into the stellar variations across each galaxy. In Table 2 we present the total fraction of FUV light from star clusters observed in each pointing. We summed up light from clusters (along the spatial direction) and compared with the total light along the slit. The fraction of light in the field is assumed to be that not found in clusters. We derive values for the fraction of light in the field portions of local starburst galaxies ranging from roughly 25% to 70%. However, our slit locations targeted UV-bright clusters, and whenever possible orientations were chosen to maximize the number of such clusters in the slit. Thus, the particular locations observed in each galaxy are biased *against* the field. The field fractions presented in Table 2 represent lower limits to the field contribution (and an upper limit to the cluster contribution) in the FUV and are roughly consistent with the ∼50%–80% field contribution derived by Meurer et al. (1995) when considering nearby starbursts in their entirety. Below we briefly describe the spatial cuts for each sample galaxy.

Mrk 33.—There are field regions on either side of, and between, two luminous UV regions that contain multiple clusters.

He 2-10.—We previously made a detailed study of starburst region A (Chandar et al. 2003). Along the spatial direction of our slit, there are five individual compact clusters on an elevated background at UV–optical wavelengths. The nature of this diffuse field light was investigated and found to include a significant population of massive stars. This population could arise in a large number of lower mass compact clusters or from diffuse SOBAs. Because the density of putative lower mass clusters would have to be very large, we concluded that SOBAs formed coevally with the compact clusters were likely the main stellar contributor to the massive star–rich field.

NGC 1741.—The field region in this galaxy includes a broad, low-level component (see Fig. 1).

NGC 3125.—There is some diffuse UV emission observed between three bright clusters. The field includes a number of faint peaks.

NGC 3310.—The spatial cut of this spiral galaxy shows a multitude of peaks. Based on the definition given in § 2.3, we detect 10 clusters. The field region includes a number of very faint peaks.

NGC 4214.—In Figure 2 we show an enlargement of the spatial profile along the STIS slit for part of the field in NGC 4214. Faint, individual peaks are clearly seen. The field appears qualitatively similar to that in NGC 5253, where a number of bumps and wiggles are seen on a broad, elevated UV background.

NGC 4449.—This galaxy is similar to NGC 3310 in the spatial direction, where a relatively large number (12) of individual clusters are found, and the field includes additional, faint peaks.

NGC 4670.—This galaxy has a profile similar to that seen in He 2-10: there is a somewhat peaked plateau of diffuse emission, with bright clusters superposed. There is, however, slightly more structure seen in the field of NGC 4670 than that in He 2-10.

NGC 5253.—This galaxy was studied by Tremonti et al. (2001). There is an elevated UV background, with a number of small peaks (included in the field) and larger peaks (defined as individual clusters).

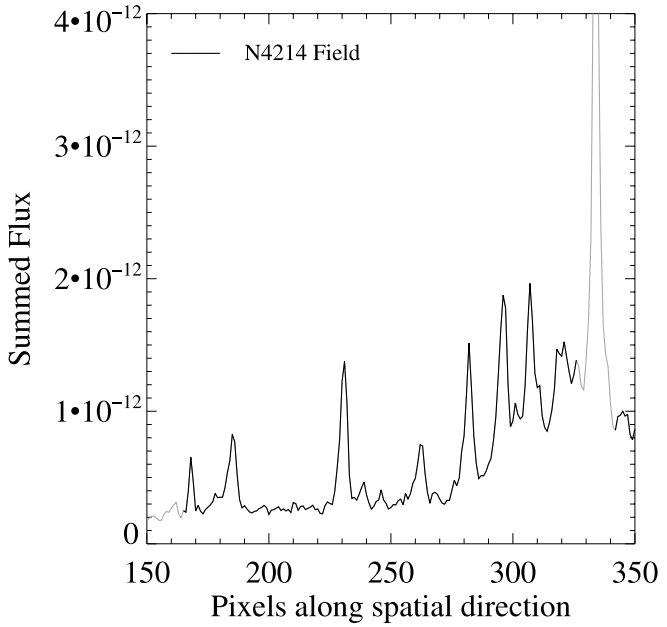


FIG. 2.—Enlargement of the flux along the spatial direction for a portion of NGC 4214 (*gray*) containing some field regions (*black*). This figure shows how the field light is not smooth but contains a number of faint peaks and valleys.

NGC 5996.—In addition to the targeted central cluster, a couple of other fainter clusters and field regions are observed in the slit.

NGC 7552.—There are two bright clusters on an elevated background in the slit, with some field portions in between.

Tol 1924−416.—There is one very luminous cluster, plus one fainter one. The field consists of a number of low-level bumps and wiggles.

3. COMPLEMENTARY ARCHIVAL WFPC2 IMAGES

3.1. *Data and Reduction*

To further constrain properties of the field regions studied in this work, we downloaded available archival WFPC2 images for our target galaxies. These allow the study of the stellar populations along the slit at different wavelengths, as well as providing a broader view of the stellar populations in our target galaxies, and not just the pointings targeted by our STIS long-slit spectra. Because much of the available archival data are not very deep or do not include observations in several filters, we restrict the WFPC2 image analysis to the three closest galaxies, NGC 4214, NGC 4449, and NGC 5253, where individual stars can easily be detected and the UV spectra are least subject to issues related to distance bias. These three target galaxies all have observations in filters that can be converted to Johnson-Cousins *U*, *V*, and *I*. In Table 3 we compile information on these galaxies and on the archival WFPC2 observations used in this work. Images were processed through the *HST* on-the-fly calibration pipeline (which automatically selects the most up-to-date calibration files during processing). Multiple images were combined to eliminate cosmic rays.

We ran the object-finding algorithm SExtractor (Bertin & Arnouts 1996), to locate all objects (individual stars, clusters, and a handful of background galaxies) in the F336W images (the closest match to the wavelength range of our STIS observations). We used a threshold of 3 σ above the local background level, which upon visual inspection appeared to detect all obvious sources. In general, a detection that is the mean of the local background plus 3 times the standard deviation (σ) of this background eliminates random surface brightness fluctuations and leads to detection of actual objects. The F336W filter has a significant red leak, causing a fraction of an object's flux longward of 4000 Å to be detected in this filter. Biretta et al. (2000) show that the red leak in this filter is generally $\lesssim$5% of the total flux for stellar populations dominated by K3 V or earlier type stars, which is appropriate for the majority of objects observed in the three closest galaxies. However, one cluster in NGC 5253 is of particular interest, cluster 5 from Calzetti et al. (1997). This is a highly extincted, very young cluster, which emits strong thermal radio emission but is also seen in optical/ultraviolet images. Note that the exact photometry for this single object does not affect our overall conclusions.

3.2. *Photometry*

Aperture photometry was obtained using the PHOT task in DAOPHOT (Stetson 1987). It has been established that aperture corrections in different *HST* WFPC2 filters show very little difference with object size (Holtzman et al. 1995; Larsen 1999). Thus, we used a small aperture radius ($r = 3$ pixels) to determine object colors, in order to minimize contamination due to neighboring sources and the impact of uncertainties in the background determination when fainter object light is included. However, there is a significant fraction of light outside this radius, which varies based on how extended an object is and directly impacts the total magnitude measurements. In order to measure aperture corrections for our sources, we first measured the sizes of all detected objects using Larsen's (1999) ISHAPE routine. Details of size measurements are given below. Since the sources have a large range of sizes, which leads to very different aperture corrections, we linked the aperture corrections to the measured size for each object. We used the previously measured aperture corrections from Larsen & Brodie (2000) for ISHAPE KING30 models (for $\Delta m_{3\rightarrow5}$ and $\Delta m_{5\rightarrow30}$), which are compiled in their Table 1. These values are given for discrete values of the measured FWHM in pixels. We fitted a second-order polynomial to these values and used this equation to calculate aperture corrections for each object individually.

TABLE 3
ARCHIVAL WFPC2 DATA

GALAXY	E_{B-V} FOREGROUND[a]	FILTER EXPOSURE TIME(s) F336W (*U*)	F555W (*V*)	F814W (*I*)
NGC 4214.....	0.022	2 × 900	2 × 600	2 × 600
NGC 4449.....	0.019	2 × 260	1 × 200	1 × 200
NGC 5253.....	0.056	2 × 260	1 × 200	2 × 200

[a] Foreground, Milky Way extinction from the Schlegel et al. (1998) maps.

Charge transfer efficiency corrections were performed as described in Dolphin (2000).[8] The corrected instrumental magnitudes were converted to standard Johnson-Cousins *U*, *V*, and *I* magnitudes. Using equation (8) and Table 7 of Holtzman et al. (1995), the magnitudes were derived iteratively using WFPC2 observations in two filters.

3.3. *Size Measurements*

Intrinsic sizes for our entire object sample were measured using the ISHAPE routine. A detailed description of the code is given in Larsen (1999), along with the results of extensive performance testing. Essentially, ISHAPE measures intrinsic object sizes by adopting an analytic model of the source and convolving this model with a (user supplied) point-spread function (PSF) and then adjusting the shape parameters until the best match is obtained. King model profiles with concentration parameters of $c = 30$ were convolved with a PSF and fitted individually to each object. ISHAPE estimates the FWHM of each cluster (in pixels), which was then converted to the half-light (effective) radius, $r_{\rm eff}$, as described in the ISHAPE manual. The input PSF to this algorithm is crucial. We created a PSF by hand selecting stars in the image and then compared the results with those of a subsampled Tiny Tim PSF (when the Tiny Tim PSF was used, convolution with the WFPC2 diffusion kernel was implemented). We found that the size estimates from ISHAPE using these two PSFs differed by less than 20%. Final measurements were made using the Tiny Tim PSF, since this is easily reproducible. A single PSF was generated for the PC CCD, and one for the WF CCDs. We assume that objects with $\Delta_{\rm FWHM}$ ($\rm FWHM_{measured} - FWHM_{PSF}$) of 0.2 pixels or less are unresolved point sources.

4. ANALYSIS

4.1. *Deriving Stellar Properties*

One way to assess (any) differences between clusters and the field in local starbursts is to quantify the stellar content of each.

[8] See http://www.noao.edu/staff/dolphin/wfpc2_calib for updated calibrated information.

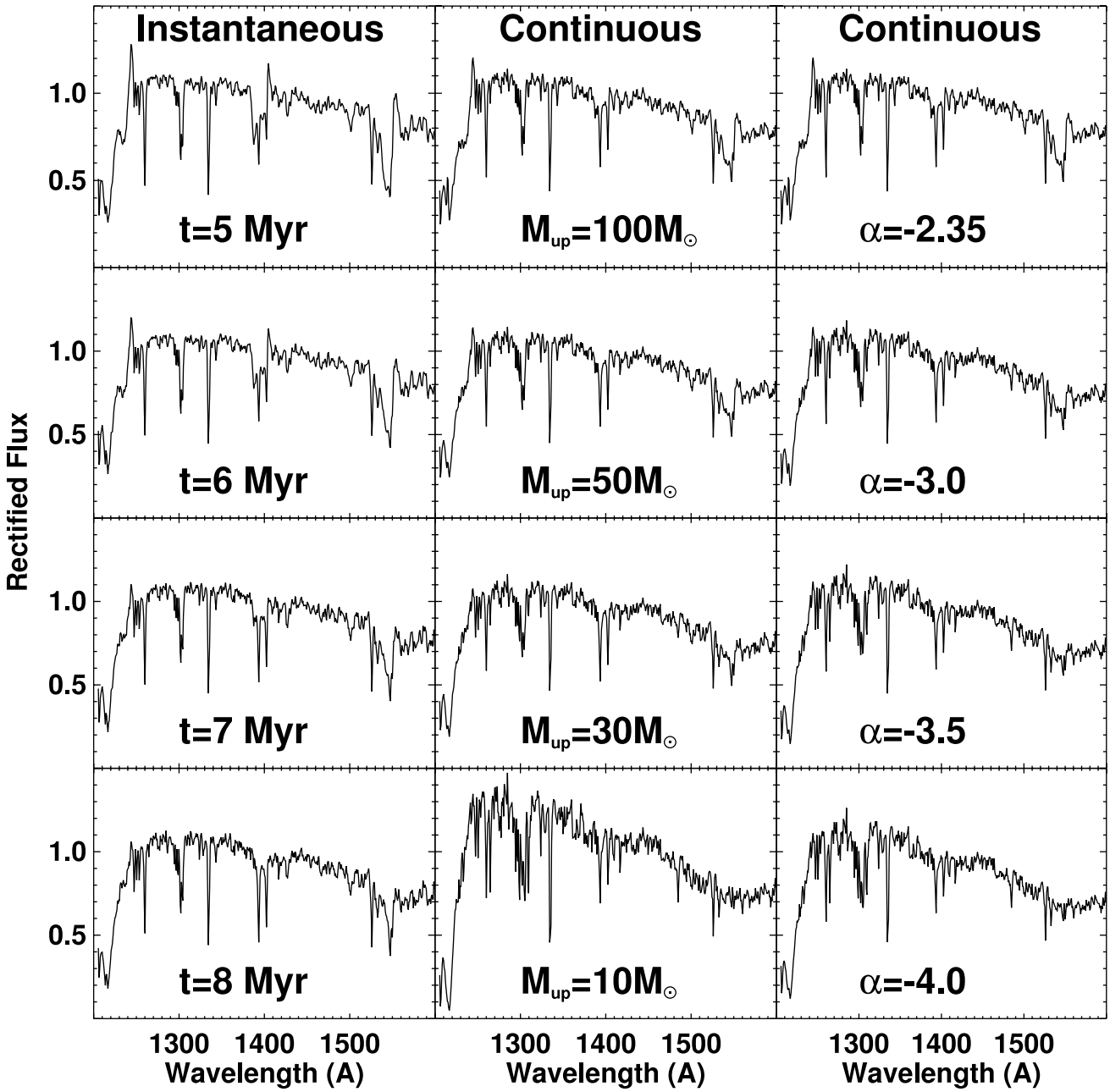


FIG. 3.—Example spectra from various Starburst99 models considered in this work. The strength of the Si IV λ1400 and C IV λ1550 wind features, plus other diagnostics, provides excellent constraints on the massive star content in nearby galaxies. The left panels show the effect of aging on the UV spectrum of an instantaneous burst stellar population, with $M_{up} = 100\,M_{\odot}$. The middle panels show the variations in a continuous star formation episode when the upper mass cutoff for the IMF is lowered from 100 to 10 $M_{\odot}$. The right panels show UV spectra for continuous star formation models with different IMF slopes, α. The duration for the continuous star formation shown in the middle and right panels is 50 Myr.

Is the field lacking in massive stars relative to neighboring clusters? The answer to this question can be used as a starting point to study the composition of galaxies and make inferences concerning the properties of star formation. One of the main advantages of using UV spectroscopy to assess the differences between stellar content in clusters and the field is the short timescales over which massive stars evolve. To illustrate the diagnostic power of UV spectroscopy in assessing massive star content, in Figure 3 we present example spectra from various Starburst99 models that clearly show the effect massive stars have on composite FUV spectra of stellar populations, particularly on the N V λ1240, Si IV λ1400, and C IV λ1550 broad P Cygni profiles.

In order to make a quantitative comparison between the stellar populations dominating clusters and field regions, we created composite "cluster" spectra, which are the unweighted sum of multiple clusters. When there were a number of clusters available, we combined them by luminosity, making an arbitrary separation between bright and faint clusters, depending on specifics of cluster characteristics (luminosities) within a given galaxy. In general, since younger clusters tend to be more luminous than older ones of comparable mass, this will roughly divide clusters by age. To derive quantitative cluster parameters, we then compare dereddened (reddening discussed below) cluster spectra to a grid of instantaneous burst Starburst99 models (Leitherer et al. 1999), and we record the results in

TABLE 4
COMPARISON OF MEAN AGES (Myr) OF DOMINANT CLUSTER VERSUS FIELD STELLAR POPULATIONS

Galaxy	Bright Clusters	Faint Clusters	Field
He 2-10	$4.5^{+0.4}_{-0.6}$	...	$4.6^{+0.5}_{-0.7}$
Mrk 33	...	$5.0^{+0.5}_{-0.5}$	$6.0^{+0.5}_{-0.5}$
NGC 1741	$3.0^{+0.5}_{-0.6}$	$6.0^{+0.5}_{-0.5}$	$7.0^{+0.8}_{-0.4}$
NGC 3125	...	$3.0^{+0.5}_{-0.5}$	$8.0^{+1.4}_{-0.4}$
NGC 3310	$5.0^{+0.5}_{-0.5}$	$7.0^{+0.8}_{-0.4}$	$8.0^{+1.2}_{-0.3}$
NGC 4214	$4.0^{+0.5}_{-0.5}$	$7.0^{+0.9}_{-0.4}$	$9.0^{+0.6}_{-1.0}$
NGC 4449	...	$5.0^{+0.5}_{-0.5}$	$7.0^{+1.2}_{-0.6}$
NGC 4670	$7.0^{+0.7}_{-0.4}$	$5.0^{+0.6}_{-0.5}$	$6.0^{+0.5}_{-0.5}$
NGC 5253	...	$4.0^{+0.4}_{-0.4}$	$7.0^{+0.8}_{-0.4}$
NGC 5996	$5.0^{+0.4}_{-0.4}$	$6.0^{+0.8}_{-0.4}$	$6.0^{+2.2}_{-0.6}$
NGC 7552	$5.0^{+0.5}_{-0.5}$	...	$6.0^{+0.6}_{-0.4}$
Tol 1924−416	$1.0^{+0.5}_{-0.8}$	...	$7.0^{+1.0}_{-0.3}$

NOTES.—The ages in Myr and associated uncertainties have been derived by comparing the observations with instantaneous Starburst99 models, assuming a Salpeter IMF and upper and lower mass cutoffs of 100 and 1 $M_{\odot}$, respectively. The uncertainties were determined by using the bootstrap technique as described in Tremonti et al. (2001).

Table 4. Instantaneous burst models are appropriate for compact clusters, since they are coeval stellar populations with small crossing times (<0.1 Myr) compared with the models. While instantaneous burst models are not an ideal physical representation of field regions extending over hundred of parsecs, they provide a consistent way to compare the stellar content of clusters and the field. Because we are working in the UV, the field spectra, even though they probably contain a mix of ages, will be dominated by signatures of the youngest stellar populations. In § 5.5.2 we compare our field regions with continuous star formation models.

Starburst99 models have been optimized to reproduce many spectrophotometric properties of galaxies with active star formation. Details of the input stellar parameters to Starburst99 can be found in Leitherer et al. (1999); here we briefly summarize the model parameters used in this work. The Starburst99 UV spectral library is available for two metallicities: solar and LMC/SMC ($\sim\frac{1}{4}$ solar). In general, we used the metallicity model that provides the closest match to a given galaxy's abundance (tabulated in R. Chandar et al. 2005a, in preparation). However, for some galaxies the abundance is in between the two models. For these, we compared the results from both abundance models and adopted the one that resulted in the better fit (lower χ^2). In general, age estimates for individual clusters are in good agreement between the two models.

For the instantaneous burst models, we adopted a standard Salpeter (1955) initial mass function (IMF), with lower and upper masses of 1 and 100 $M_{\odot}$, respectively. Arguments in favor of a Salpeter IMF are summarized in Leitherer (1998), and a discussion of various studies available in the literature can be found in Tremonti et al. (2001). High mass-loss rates, as required by stellar evolution, were assumed (Meynet et al. 1994).

In order to determine intrinsic properties for a stellar population, the one-dimensional spectra must be corrected for the effect of (foreground) Galactic extinction, as well as for the dust obscuration intrinsic to the starburst itself. We assume foreground extinction values from the Schlegel et al. (1998) maps and adopt the extinction curve of Fitzpatrick (1999). To determine the reddening internal to the starburst itself, we compared the observed continuum of each cluster and field spectrum with stellar evolutionary models. The intrinsic FUV spectral distribution of young, unobscured single stellar populations follows a power law, with effective spectral index β, where $F_{\lambda} \propto \lambda^{\beta}$. Any deviation of the power-law exponent from that predicted by theoretical models is assumed to be due to the effects of dust. The intrinsic UV spectral energy distributions (SEDs) of any young (<10 Myr) starburst population are typically near $\beta \sim -2.6$. The fit for β was performed over the spectral region 1240–1600 Å. To account for the spectral features (which are mostly in absorption), we performed the fit iteratively with rejection thresholds set at 2 σ for the lower bound and a 3.5 σ upper bound.

We determined which model age provided the best fit to our clusters and field spectra by comparing the (foreground+intrinsic) extinction-corrected object spectra with instantaneous burst models from Starburst99 with ages of 1–100 Myr in steps of 1 Myr. Model fitting closely follows the techniques developed by Tremonti et al. (2001), and the reader is referred to that work for details. Briefly, in order to maximize the sensitivity of χ^2 to spectral regions most sensitive to the age and stellar content of the starburst, each pixel in the spectrum is classified as belonging to either the continuum, an interstellar line, or a stellar wind line (based on the detailed line analysis of de Mello et al. 2000). These were then assigned weights, with interstellar lines being given a weight of 0, continuum a weight of 1, and stellar wind lines a weight of 10. Because nearly all of the features that are sensitive diagnostics of the age of a stellar population also have some interstellar contamination, the interstellar cores of the N V λ1240, Si IV λ1400, and C IV λ1550 lines were also masked out. This effectively eliminates the interstellar medium (ISM) from consideration and relies only on stellar signatures to derive their properties. The routine returns the best-fit age (minimum χ^2), which is given in Table 4.

To quantify errors associated with our best-fit models, we utilized the bootstrap technique. The residuals of the best fit were randomly resampled and added to the model spectrum, and then rerun through the automated fitting routine 1000 times. The error bars associated with the 90% confidence interval were derived from a histogram of the derived ages. The age uncertainties are also given in Table 4. For clusters, ages can be derived to within $\pm$1 Myr, highlighting the strong effect that massive, short-lived stars have on the UV spectrum.

4.2. *Summary of Model Fitting by Galaxy*

Figure 4 shows composite cluster and field spectra for each galaxy in our sample. The results from comparison with instantaneous burst models are given in Table 4 and discussed generally below. Note that the figures, analysis, and discussion are based on our first definition of the field, where we have included all regions within 3 σ of the local background, since this is a more conservative approach and does not include obvious star clusters. However, we have verified that the results presented here do not change substantially for the second field definition in each galaxy.

Mrk 33.—Figure 4 shows the composite cluster and field spectra for Mrk 33. The field has weak signatures of massive O stars and has a best-fit age of 6 Myr when compared with instantaneous burst models. This is slightly older than found for the composite cluster spectrum. In general, we found that separating clusters into a bright and faint category kept any individual cluster from severely biasing the luminosity-weighted age of the composite cluster spectra.

He 2-10.—Studied in a previous paper (Chandar et al. 2003), the main starburst region (A) shows individual compact clusters on an elevated background at UV–optical wavelengths. The

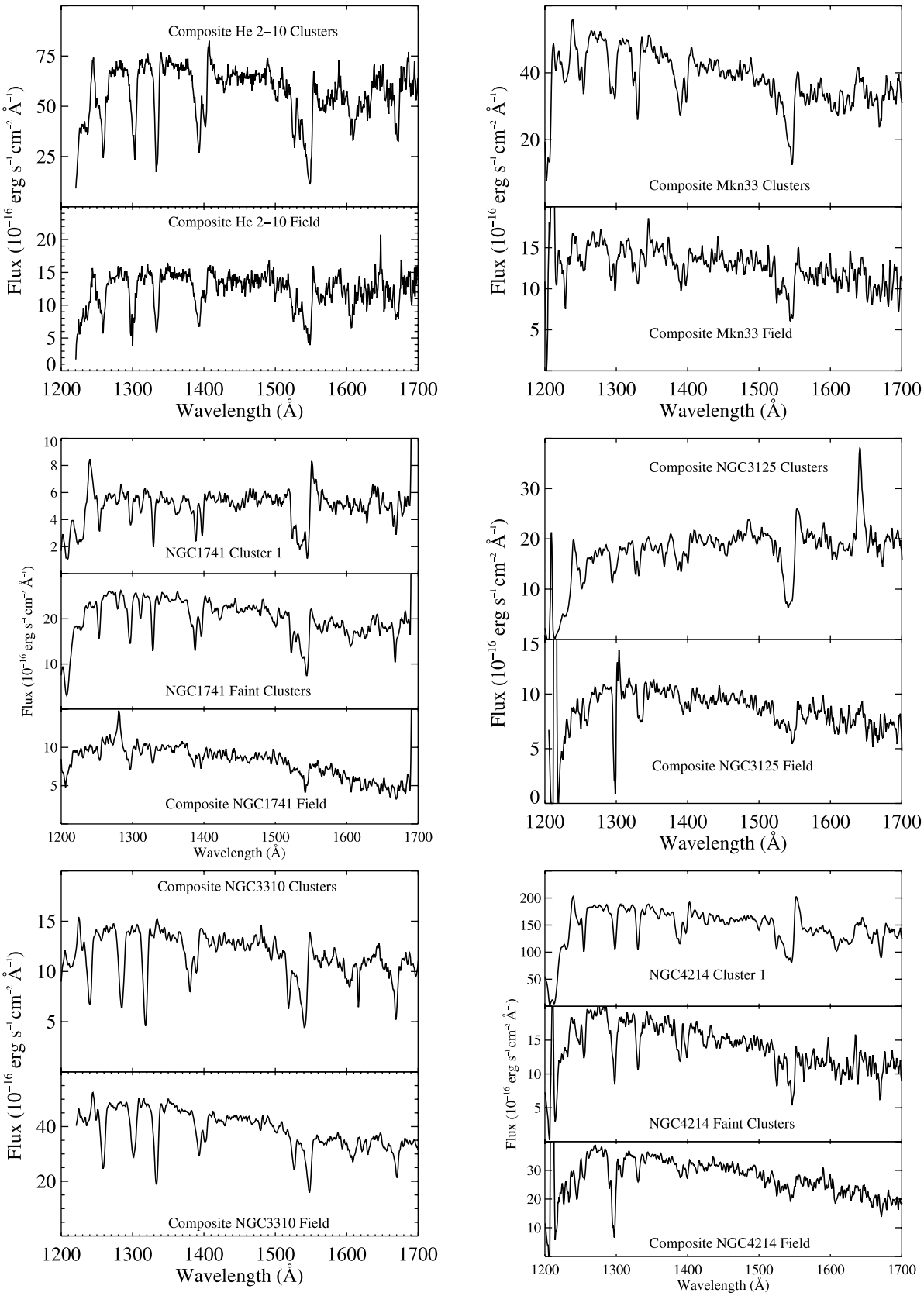


FIG. 4.—Unweighted sum of star cluster spectra and summed field spectra extracted for our target galaxies.

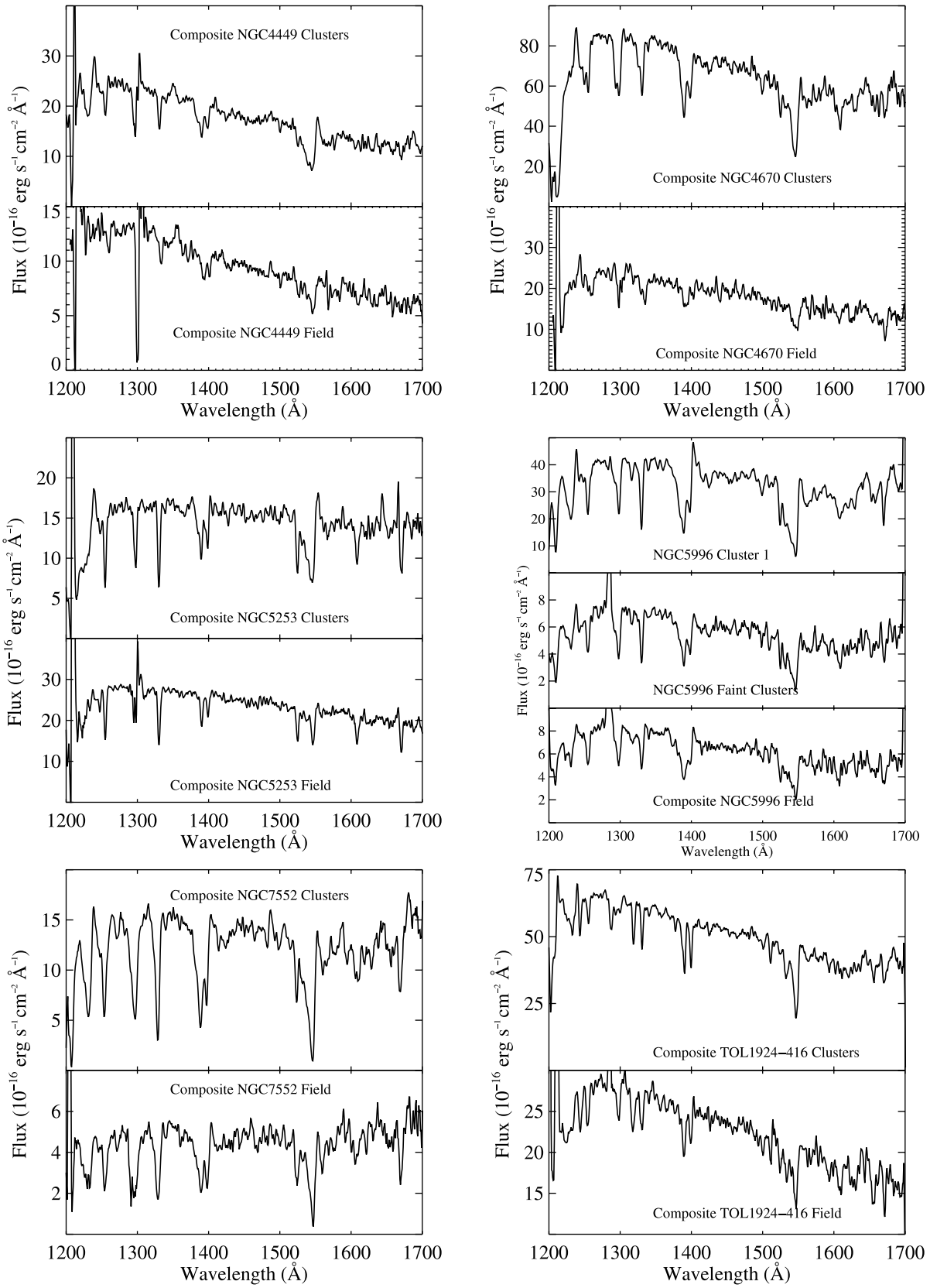


FIG. 4.—*Continued*

nature of this diffuse field light was investigated and found to include a significant population of massive stars. We concluded that a large number of lower mass compact clusters or diffuse SOBAs could be responsible. The tails of this diffuse emission extend out ~100 pc from starburst A. The diffuse field light is fainter but shows the same spectral signature as that in starburst region A. Therefore, we see the signature of massive stars forming in the "field" in this actively starbursting galaxy.

NGC 1741.—Figure 4 shows a sequence of three "composite" stellar populations. The top panel shows the most luminous cluster in our slit, cluster 1, the middle panel is an average of fainter clusters 2, 3, and 4, while the bottom panel shows the field spectrum. There is a clear gradient in the stellar populations in this galaxy, as traced by the strength of the stellar wind lines: these are strongest in luminous cluster 1, weaker in clusters 2, 3, 4, and weaker still in the field. These observations suggest an age sequence, which is quantified in Table 4.

Cluster 1 is quite young, with a best-fit age of 3 Myr. The other three clusters all have ages of 6 Myr. The field has the oldest composite age of 7–8 Myr, depending slightly on which metallicity model is adopted. Regardless, there is no obvious signature from the most massive stars in the field region.

NGC 3125.—The average spectrum of the two most luminous clusters shows significantly stronger wind lines (in particular N v λ1240 and Si iv λ1400) relative to the field. Cluster NGC 3125-1 also shows strong WR signatures, including the N iv] $\lambda\lambda$1487,1718 lines and the He ii λ1640 line typically found in WN stars (for a detailed derivation of the properties for this unusual cluster see Chandar et al. 2004). Fits to Starburst99 instantaneous burst models give mean ages of 3 Myr for both clusters and 8 Myr for the field.

NGC 3310.—The five brightest clusters have a mean age of 5 Myr, and five faint ones have a mean age of 7 Myr. The field has a best-fit age of 8 Myr.

NGC 4214.—The brightest cluster has strong wind lines and a young age (4 Myr). When we average the individual fainter cluster spectra, we find that these objects are not only fainter, but they are also older on average, with a mean age of 7 Myr. Our best fit to the field gives an age of 8 Myr.

NGC 4449.—The mean cluster spectrum shows P Cygni profiles and has a formal age of 5 Myr. The field shows little evidence for the presence of massive stars and has a best-fit age of 7 Myr.

NGC 4670.—The most luminous cluster, NGC 4670-1 is 7 Myr old. Three fainter clusters (2, 3, 4) are coeval, with ages of 5 Myr. Note also that these fainter clusters are located very close to one another, while cluster 1 is located slightly farther away. The composite field shows the weak signature of massive stars and has a mean age of 6 Myr old when compared with instantaneous burst models.

NGC 5253.—Tremonti et al. (2001) find a difference in the mean ages of the composite cluster and field spectra. Redoing the extraction independently, we find a mean age for the nine extracted clusters of 4 Myr and a mean age for the field regions of 7 Myr, similar to the earlier results.

NGC 5996.—The brightest cluster is also the youngest, at 5 Myr. The strength of the wind lines (particularly the Si iv λ1400 feature) in the composite faint cluster spectrum and the field establishes that massive stars reside in both the faint clusters and the field, even though these appear to be somewhat older than the brightest cluster. N v λ1240 and C iv λ1550 are slightly more pronounced in the faint clusters than the field, so these may contain somewhat more massive stars than the field.

NGC 7552.—The two bright clusters have a mean age of 5 Myr, while the field appears slightly older, at 6 Myr.

Tol 1924−416.—The brightest cluster has an age of 1 Myr, while the youngest stellar population contributing to the UV field light has an age of 7 Myr.

4.3. *Radial Profiles*

Radial profiles for objects in nearby galaxies can be used to determine whether an object is extended or not. If an object is resolved, it is likely a cluster or group of stars; however, unresolved objects can be either stars, chance superpositions, surface brightness fluctuations, or compact clusters. Although size estimates are typically made from imaging, here we attempt to also use the information along the spatial direction of the slit to determine whether clusters and bumps/wiggles in the field are resolved, and from there reach some conclusion concerning the nature of the diffuse UV light. This is particularly valuable since STIS pixels sample even smaller scales ($0\farcs025$ pixel^{-1}) than the PC ($0\farcs0455$ pixel^{-1}) CCD on WFPC2.

To measure the FWHM of bumps/wiggles in the field, we compare with the FWHM measurement of a bright star (GD 71) observed with the same grating and slit combination. We measure the FWHM of star GD 71 to be ~$0\farcs08$ and take this to represent a point source. Because the size estimates for the faint peaks in the field are likely not very accurate, we only determine whether these appear resolved or not, relative to the measurement of GD 71. We discuss the results of this exercise in § 5.4.

5. DISCUSSION

5.1. *Is Scattered UV Light Responsible for the Field?*

Could the scattering of UV photons explain the presence of diffuse UV emission in local starburst galaxies? In this scenario, UV photons originate in young stars embedded in the massive clusters. Since most of the nonionizing UV radiation produced in star-forming regions escapes the local cluster (e.g., Misiriotis et al. 2001; Hippelein et al. 2003), it is free to be scattered by interstellar dust. Recent GALEX UV images of nearby spiral galaxies clearly show the presence of diffuse UV emission between spiral arms (e.g., M101; Popescu et al. 2005) and at large galactocentric radii (e.g., M33, M31, and M83; Thilker et al. 2005a, 2005b). When combined with observations at longer wavelengths, the SEDs of spiral galaxies are well reproduced by galaxy components that include a layer of diffusely distributed cold dust (e.g., Popescu et al. 2000). Far-IR and submillimeter imaging of nearby spiral galaxies has directly shown that this layer of cold dust covers the entire extent of the disk (e.g., Haas et al. 1998; Hippelein et al. 2003; Popescu et al. 2005). In M101, a comparison of GALEX UV and *ISO* far-IR images showed that the ratio of UV/far-IR emission varies between arm and interarm regions (Popescu et al. 2005). These differences are consistent with the interarm UV emission being scattered light originating from massive stars in the spiral arms. Similarly, the diffuse FUV emission observed beyond the Hα disk in M33, M31, and M83 (Thilker et al. 2005a, 2005b) is interpreted as nonionizing UV radiation escaping from the outermost H ii regions and then scattering off dust grains farther out in the disk.

Could the diffuse UV light observed in local starburst galaxies result from such scattering of UV photons? Scattering by dust can change the original spectral shape (i.e., make the spectrum appear bluer) but cannot add or subtract narrow spectral features, such as P Cygni profiles. In this work we have shown that the young, massive stars that dominate the UV flux from clusters have an O-type spectrum, with prominent P Cygni profiles. By contrast, the UV light originating in the field shows

a B-type stellar spectrum. Because the spectra from the two environments have *different* stellar features, massive stars powering the luminous clusters are not the original source for any UV photons scattering off dust grains. However, if lower mass, B star–dominated clusters are found in the field, we cannot rule out the possibility that photons escaping from these lower mass clusters are scattered and thus produce the field UV light. Regardless, the differences in spectral features observed between the field and clusters demonstrate that the UV emission in each environment originates in a *different stellar population*.

How can our evidence that the diffuse UV light in starburst originates in a (faint) stellar population be reconciled with the claim that the diffuse interarm UV light in M101 is due to scattering off dust grains? First, the geometry and distribution of dust in large spiral galaxies may differ substantially from that in dwarf systems such as those that often host starbursts. Second, Popescu et al. (2005) point out that even in the most extreme interarm regions discrete sources of UV emission are observed in full-resolution GALEX images. Given the low resolution of the GALEX images (6″ FWHM) with respect to *HST*, it is plausible that some fraction of the diffuse interarm emission in M101 arises from a dispersed stellar population rather than from scattering due to dust. For example, the GALEX images are not sufficiently deep (and do not have the spatial resolution) to detect individual B stars (which are a plausible contributor to the diffuse UV field light). Rather, these observations are appropriate for studying stellar complexes that have sizes of many tens to hundreds of parsecs at the distance of M101. An analysis of WFPC2 images for NGC 4214, NGC 4449, and NGC 5253 clearly reveals a population of dispersed blue point sources, which are consistent with a population of B supergiants (§ 5.3). We suggest that deep UV imaging of interarm regions in spiral galaxies, with sufficient depth to reveal the presence of individual B stars, could resolve whether the diffuse UV emission in M101 arises primarily from a diffuse layer of dust or from a discrete stellar population.

5.2. *General Summary of the Stellar Content in Field Regions of Starbursts*

5.2.1. *FUV Slope Measurements*

In Table 5 we compile slopes, β, measured for the composite field and cluster spectra after correction for foreground extinction, but with no correction for extinction due to the host galaxy. Details of the β measurements were provided in § 4.1. The main uncertainties in the values of β come from the fact that a power law does not always provide a good fit to the data, mostly due to line blanketing in the spectra (although we have excluded the most severely line-blanketed spectral regions longward of 1640 Å).

In general, the intrinsic slope of a stellar population becomes redder with age. However, a comparison of the slopes for single stellar populations younger than ~10 Myr (typical ages of clusters observed in our starburst galaxies) with those for continuous formation models that fit our data shows that both have similar values. For example, a continuous star formation model with Salpeter IMF and upper mass cutoff of 30 $M_{\odot}$ has an intrinsic slope, $\beta = -2.5$ (see § 5.5.2 for a discussion of continuous star formation models and their comparison with the data). Because the dominant/youngest UV populations in the clusters are somewhat younger than those in the field (as discussed in detail below), one might expect that the intrinsic slope for the clusters is somewhat bluer than for the field.

In Table 5, however, β measurements for the field appear comparable to or bluer (steeper) than for half (6/12) of the field spectra when compared with the composite cluster spectra in the same galaxy. Because the spectral features in the UV allow us to precisely age-date the stellar populations in the clusters and the field, we know that the dominant stars in the field are generally older or less massive than those in the clusters. Therefore, one might expect that β for the clusters would be bluer than for the field. However, our study establishes that the field is not *categorically* redder than young clusters in starbursts. A more likely explanation for the observed difference in slopes between clusters and the field is extinction variations between stellar populations residing in each environment, with the field showing less reddening. Because the UV-bright clusters are quite young, it is likely that they still have at least some residual natal ISM and dust surrounding them, leading to redder slope measurements.

TABLE 5
Comparison of Continuum Slopes in Cluster versus Field Stellar Populations

Galaxy	FUV Slope (β)[a]		
	Bright Clusters	Faint Clusters	Field
He 2-10	−1.66	...	−0.59
Mrk 33	...	−1.89	−1.37
NGC 1741	−1.18	−1.75	−2.27
NGC 3125	...	+0.12	−0.84
NGC 3310	−0.91	−1.21	−1.37
NGC 4214	−1.18	−2.05	−0.94
NGC 4449	...	−3.02	−2.12
NGC 4670	−1.95	−1.65	−2.14
NGC 5253	...	−1.03	−1.48
NGC 5996	−2.02	−2.42	−2.74
NGC 7552	−0.87	...	+0.11
Tol 1924−416	−2.27	...	−2.02

[a] The FUV slope, β, measured after correcting for foreground extinction. Typical uncertainties on β measurements are ±0.1.

The bluer, less reddened slopes found in the field regions of some local starbursts when compared with star clusters have implications for the overall extinction estimates derived for high-redshift galaxies. This is particularly important when UV spectra of whole high-z galaxies are compared with narrow-slit or small-aperture UV spectra of local star-forming galaxies. Inferences of differences in stellar population compositions and/or extinction characteristics may stem from the fact that the UV spectrum of the local galaxy is only targeting one component (e.g., one cluster) of the entire star-forming region.

5.2.2. *Characterizing the Field Stellar Population*

We find that the overall stellar content in our observed STIS field regions of nearby starburst galaxies can be divided into three broad categories: the clear presence of O stars, a clear lack of O stars, and an intermediate class showing a weak signature of O stars. He 2-10 is unique to our sample, with the youngest mean field stellar population of any sample galaxy, clearly showing the signature of O stars. The other extreme includes seven galaxies, which show field spectra lacking in the most massive stars (absent P Cygni profiles), similar to that found by Tremonti et al. (2001) for NGC 5253. This category also includes NGC 1741, NGC 3125, NGC 3310, NGC 4214, NGC 4449, and Tol 1924−416. Table 4 shows that these have best-fit ages of ≥7 Myr, and inspection of the field spectra in Figure 4 confirms the lack of massive stars. The third category comprises Mrk 33, NGC 4670, NGC 5996, and NGC 7552, which

TABLE 6
MEAN STAR FORMATION RATES DERIVED FOR STIS FIELD REGIONS

Galaxy	Pixels[a]	E_{B-V}[b]	L_{1500}[c] (ergs s^{-1} Å^{-1})	SFR[d] ($M_\odot$ yr^{-1} kpc^{-2})	Number of O Stars[e]
Mrk 33	181	0.18	4.7E38	1.8	490
NGC 1741	221	0.04	6.7E38	0.3	720
NGC 3125	365	0.28	3.8E38	2.7	410
NGC 3310	623	0.18	5.6E38	1.7	590
NGC 4214	533	0.24	3.7E37	2.9	40
NGC 4449	298	0.11	5.6E36	0.4	10
NGC 4670	264	0.06	1.0E38	0.6	110
NGC 5253	633	0.18	2.4E37	2.4	20
NGC 5996	65	0.00	2.2E38	0.5	230
NGC 7552	147	0.41	1.5E39	8.0	1600
Tol 1924−416	271	0.08	9.7E38	0.9	1000

[a] Total number of pixels summed up in the spatial direction for each field region.
[b] Reddening derived using the starburst obscuration curve from the difference in the model slope (−2.5) and the observed slope of the field after correction for foreground reddening.
[c] Extinction-corrected luminosity at 1500 Å measured from the STIS spectra. We use the E_{B-V} values quoted in the third column.
[d] Star formation rate. We have assumed a standard Salpeter IMF ($\alpha = -2.35$) and an upper mass cutoff for the IMF of 100 $M_\odot$. The age for the continuous star formation model has been fixed at 50 Myr.
[e] Number of O stars predicted by Starburst99 continuous star formation models (assuming a standard Salpeter IMF and $M_{up} = 100\ M_\odot$) to reside in the field region given the mean SFR given in the fifth column.

have mean field ages of 6 Myr and show weak signatures of O stars.

The closest galaxies (i.e., those within 4 Mpc; NGC 5253, NGC 4214, and NGC 4449), where we have the best spatial resolution and the easiest time distinguishing low-level clusters from the field, all clearly lack broad line profiles of N V λ1240, Si IV λ1400, and C IV λ1550 that are characteristic of O star winds, in stark contrast to the composite cluster populations in each galaxy. This result holds for both field definitions, whether we are excluding all peaks above $\gtrsim 3\ \sigma$ or only excluding targeted, luminous star clusters. Therefore, we are not concerned that our definition has a priori excluded O stars from the extracted field spectra. Not surprisingly, we see more variation in the field regions of more distant galaxies. Some, e.g., NGC 3125, NGC 3310, NGC 1741, and Tol 1924−416 (all further than 10 Mpc), clearly lack the signature of massive stars and are very similar to the field spectra for the closest galaxies. Others, such as Mrk 33, NGC 4670, NGC 5996, and NGC 7552, again more distant than 10 Mpc, show weak signatures of O stars. For galaxies in the latter group, our field extraction likely includes some young, relatively massive clusters, which provide the weak O star signature. This bias with distance is not unexpected; however, it is gratifying that a number of the more distant galaxies in our sample show a result similar to the closest targets. We conclude that the field regions of local starbursts (except He 2-10) are not conducive to the formation of isolated massive stars (as suggested is occurring in the nuclear regions of M51; Lamers et al. 2002) in the random field regions covered by our long-slit pointings.

For galaxies with mean derived field ages of $\geq$7 Myr, we find that the faint clusters are only 1−3 Myr younger than the youngest stellar populations contributing to the field regions. Implications for these relatively small differences in age between the dominant stellar populations in clusters and the field are discussed in § 5.5.4.

Based on the results described above, He 2-10 appears to be unique in our sample. Because the dominant stellar population in the field formed coevally with the nearby clusters, we estimated the UV contribution of the compact clusters in starburst region A to the total UV flux. Assuming that the clusters that did not fall in our slit have the same age as those that were studied, we find that 40% of the light comes from the clusters, leaving the remaining 60% originating in the field. This is still a lower limit, since some clusters may have dissolved, but provides a firm lower limit to the amount of UV light coming from clusters in this starburst.

Our main result from analysis of the stellar content of clusters and the field regions of starbursts is that the field generally shows weaker or absent P Cygni profiles compared with clusters. Thus, the fraction of high-mass stars that are visible is smaller in the field than in the bright clusters. Here we have simply showcased this result by presenting the best-fit ages derived by comparing instantaneous burst evolutionary synthesis models with our extracted spectra. Although this is not the best physical representation of the field, it is a simple exercise that illustrates the difference in massive star content. This result in starbursts is similar to that found for O stars in the Galaxy and LMC. Van den Bergh (2004) used a catalog of Galactic O-type stars (Maiz-Apellaniz et al. 2004) and found that O-type stars in clusters and associations have earlier types (presumably larger masses or younger ages) than those in the general field. In the LMC, Massey et al. (1995) find that although massive stars are born in the field, they form more rarely in this environment than in clusters and associations.

Could our observed lack of massive field stars result from statistics, due to the relatively small areas covered by our STIS slit, or possibly due to modest star formation rates? In order to assess this possibility, we use our extracted spectra to estimate the mean star formation rate ($\overline{\mathrm{SFR}}$) implied for the field and also to predict the number of O stars expected to reside in the projected area covered by our field regions assuming a normal Salpeter IMF with an upper stellar mass limit of 100 $M_\odot$. To calculate the $\overline{\mathrm{SFR}}$ in the field regions of local starbursts, we compare our dereddened (for both foreground and intrinsic extinction) field luminosity at 1500 Å (corrected for distance) with that predicted by a continuous Starburst99 model with Salpeter IMF. The parameters used for this calculation, along with the derived field $\overline{\mathrm{SFR}}$, are compiled in Table 6. Meurer et al. (1995) used UV FOC images to estimate the star formation rate for a

number of local starbursts. If we correct their derived $\overline{\mathrm{SFR}}$ for massive stars by a factor of 2.16 to extend the IMF down to 1 $M_\odot$, we find values within a factor of $\sim$2–3 for the five galaxies in common between the two works (NGC 3310, NGC 4670, NGC 5253, NGC 7552, and Tol 1924−416); a high value for the $\overline{\mathrm{SFR}}$ in NGC 7552 is found in both works.

To assess whether sampling statistics is responsible for missing field O stars, we assume a continuous star formation episode from the Starburst99 models, appropriate for the spatially extended field regions, with Salpeter IMF, $M_{\mathrm{low}} = 1\ M_\odot$ and $M_{\mathrm{up}} = 100\ M_\odot$, and with a metallicity appropriate for each galaxy. The number of O stars in this model equilibrates after 10 Myr, and we scale the star formation rate (as calculated above) and projected area of the field regions to estimate the predicted number of O stars under these assumptions. The results are tabulated in the sixth column of Table 6. This exercise establishes that our spectra cover large enough portions of the field that, if the field IMF is the same as that for clusters, and massive stars in the field are not heavily enshrouded in dust, their signature should be clearly visible in our UV spectra.

5.3. *Photometry Results for NGC 4214, NGC 4449, and NGC 5253 and Implications*

In order to give a broader and complementary picture of the stellar content in the field regions of the closest galaxies, here we analyze photometry of the archival WFPC2 multiband imaging. This is not meant to be a rigorous examination of the stellar content. Rather, we are interested in obtaining additional information that will shed light on the nature of the field populations observed in our STIS spectra.

In Figure 5 we plot two-color and color-magnitude diagrams for sources detected in the WFPC2 CCD where our STIS slit location falls. The top panel in each figure shows the $U - V$ versus $V - I$ color-color diagram; the object colors have been dereddened by the foreground extinction values of Schlegel et al. (1998). Resolved ($\Delta_{\mathrm{FWHM}} > 0.2$ pixels) and unresolved ($\Delta_{\mathrm{FWHM}} \leq 0.2$ pixels) objects are shown by different symbols. We also show the stellar evolutionary model predictions of Bruzual & Charlot (2003) for star clusters as a function of age, with three separate metallicity models. Although local starburst galaxies tend to have LMC/SMC-type metallicity, the tracks for these lower metallicities poorly reproduced observed colors of red giant stars (Massey & Olsen 2003). The agreement between models and observations is better at solar metallicity; therefore, we include cluster tracks at this metallicity. The bottom panel in each figure plots M_V versus the $V - I$ color. None of the data have been corrected for any internal extinction.

For each galaxy, NGC 4214, NGC 4449, and NGC 5253, the resolved and unresolved points fall in the same parameter space. In general, the $U - V$ versus $V - I$ color-color diagrams of resolved objects detected in NGC 4214, NGC 4449, and NGC 5253 show a mostly young stellar population ($\lesssim$10 Myr) when compared with stellar evolutionary models of star clusters. These resolved objects continue down to relatively faint magnitudes. Inspection of the WFPC2 images suggests that some of the objects that have Δ_{FWHM} measurements greater than 0.2 pixels are actually blends of two or more stars. However, the majority of resolved objects appear to be individual sources. These resolved objects, which appear to be good star clusters plus a handful of faint background galaxies, have luminosities extending down to at least $M_V = -5$, despite their very blue colors. We also see from the location in the WFPC2 images that individual, blue point sources are dispersed throughout each starburst galaxy. The very blue colors suggest that these are young, massive stars. However, without spectroscopy, the degeneracy in optical colors makes it difficult to determine whether these are O or B stars. Based on the field signature found in our STIS spectroscopy, at least in these three galaxies, the dispersed population of blue point sources cannot be O stars. We conclude that the combination of photometry and spectroscopy supports the presence of a dispersed population of B stars in each starburst.

In the CMDs plotted in the lower panels, we do not see evidence for differences in the absolute luminosities of resolved and unresolved sources. In all three galaxies, we find unresolved sources that have absolute V magnitudes brighter than -8, which is relatively rare for individual stars. Due to their high luminosity, these may actually be superpositions, groups, or very compact clusters, and not individual stars.

Because it appears likely that any individual stars in the WFPC2 images are B rather than O stars, which have significantly longer lifetimes and could easily have formed in clusters that have since dissolved, the data do not require ongoing star formation in the field, as suggested for NGC 1705 by Tosi et al. (2001) and Annibali et al. (2003). In NGC 1705, these authors found, via comparison of the data with synthetic CMD techniques, that to account for the bluest stars in the observed CMD required a burst of star formation $\sim$3 Myr ago. If this scenario is accurate, it implies that individual massive stars are forming in the field regions of NGC 1705 and not in stellar clusters. This conclusion differs from ours, since we find no evidence for very young O stars forming in the field, and it is possible that the dispersed B star population originally formed in clusters more than 10 Myr ago. Can these different conclusions be reconciled? One possibility is that a number of the unresolved, blue objects in NGC 1705 are actually young, low-mass star clusters. In NGC 4214, NGC 4449, and NGC 5253 we find evidence for resolved and hence likely star clusters, with blue colors down to faint magnitudes. NGC 1705 is even farther away than these three galaxies, with a distance modulus $(m - M)_0$ of 28.54 ± 0.26, making it more difficult to sort out compact clusters from individual stars based on size measurements. Higher angular resolution studies of NGC 1705 could settle this issue.

5.4. *Spatial Profile Analysis and Implications for the Field Stellar Population*

In this section we use our crude fits to low-level peaks in the spatial cut to glean additional information concerning the nature of the diffuse light. Because the contribution to the field is subject to biases with galaxy distance, where relatively higher mass clusters may be "hiding" in the field of more distant galaxies, we again focus on the closest galaxies in our sample: NGC 4214, NGC 4449, and NGC 5253, all located within 4 Mpc. For local peaks within the background that can be reasonably well isolated and do not show obvious signs of being blends, we determined whether they were resolved or unresolved (precise size estimates at these low S/N values would have large uncertainties). These three galaxies show fractions of *resolved* low-level peaks in the field (typically we found $\sim$13–17 such peaks per galaxy) from $\sim$30% to 60%. Based on our measurement of the spatial profile of the star GD 71, unresolved objects have an FWHM of $\sim$0.″08. In the STIS spatial cuts, we consider a peak to be resolved if it has an FWHM measurement of 0.″09 or greater. At the distances of NGC 4214, NGC 4449, and NGC 5253, this means that compact clusters with FWHM measurements smaller than $\sim$0.7 pc would be considered unresolved. Note that when compared with the brighter peaks that we have

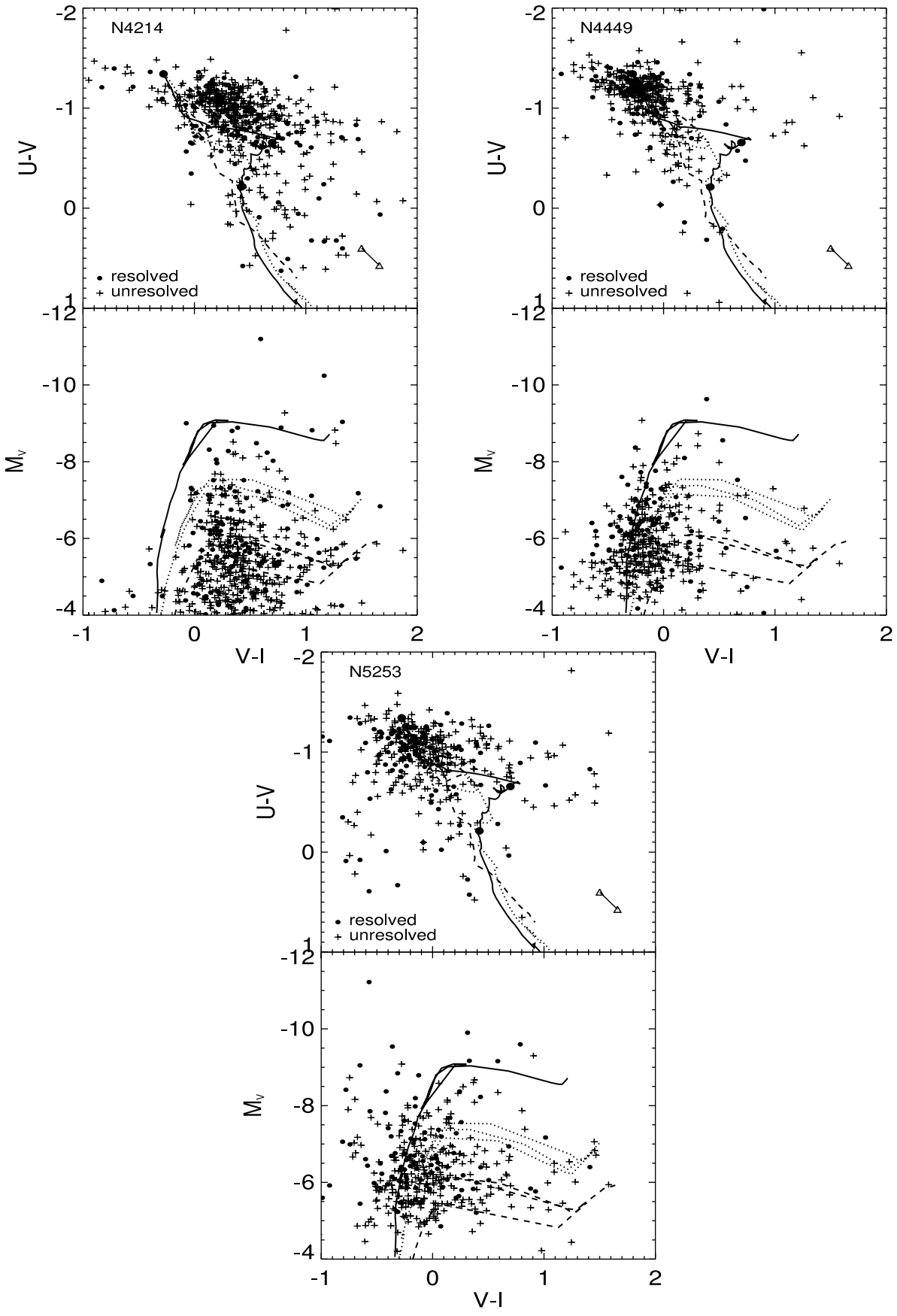


FIG. 5.—Two-color and color-magnitude diagrams for NGC 4214, NGC 4449, and NGC 5253, based on archival WFPC2 imaging. The top panels show the $U-V$ vs. $V-I$ color-color diagrams, corrected for foreground extinction only. Resolved (*circles*) and unresolved (*crosses*) sources are plotted separately. The evolution of simple stellar populations from the Bruzual & Charlot (2003) models is shown for three different metallicities: solar (*solid line*), $\frac{1}{5}$ solar (*dotted line*), and 1/50 solar (*dashed line*). The direction of the reddening vector is shown by the arrows, which represents $E_{B-V} = 0.1$. Ages of 10^6, 10^7, and 10^8 yr are shown by black filled circles along the cluster models, starting from the upper left. In the bottom panels, we show the V vs. $V-I$ CMDs. Overplotted are 30, 15, and 9 $M_\odot$ Padova stellar evolution tracks (Fagotto et al. 1994a, 1994b), with $\frac{1}{5}$ solar metallicity. [*See the electronic edition of the Journal for a color version of this figure.*]

defined as clusters, a smaller relative fraction of the faint peaks in the field are resolved within a given galaxy.

Based on the field spectral signature, we know that these are not individual O stars, although they are precisely in the flux range where we would expect to see individual O stars included in our definition of the field. Could we be seeing the continua from a dispersed B star population? To check if the observations are deep enough to detect the continua from individual B stars, we first estimated the approximate detection limit for continua in NGC 4214 from the STIS spectra (few times 10^{-16} ergs s^{-1} at 1500 Å), NGC 4449 (few times 10^{-16} ergs s^{-1}), and NGC 5253 (10^{-16} ergs s^{-1}) in our field regions. We then estimated the (unreddened) flux expected for a B0 supergiant at 1500 Å, assuming a temperature of 30,000 K and a mass of 17.5 $M_{\odot}$ from Kurucz (1993) model atmospheres. We find that in the most optimistic scenario where a single B0 supergiant has no reddening, the flux would be just above our detection limit. However, this scenario is not very likely, since lower mass B stars are much more numerous than B0 stars and because it is unlikely that such stars have no reddening, as demonstrated, for example, by a comparison of spectral type and observed color for B stars in the Humphreys (1978) catalog.

Therefore, we conclude that while some of the weaker unresolved peaks in our field spectra could be the continua from individual early B supergiants, it is unlikely that all of the unresolved peaks come from individual B stars. This does not, however, preclude a population of dispersed B stars from contributing to the continuum level observed in our UV spectroscopy of the field.

Because our calculations suggest that individual B stars are not responsible for all of the individual faint peaks seen in the field portions of our STIS spectra, it is likely that at least some of the unresolved peaks that we observe in the field regions of these local starbursts are either chance superpositions of B stars or compact star clusters. The question then becomes, are these young, low-mass clusters or older, more massive but faded clusters?

We can also use our photometry to help place limits on the properties of star clusters contributing to our STIS spectra, since it is possible to match individual sources seen in archival *U*-band WFPC2 images with the objects in our slit. If we restrict the object samples in the WFPC2 images to those within 50 pc of the STIS slit, we set approximate detection limits $M_V = -5.8$, -5.3, and -5.9 for NGC 4214, NGC 4449, and NGC 5253 respectively, from available WFPC2 imaging. A comparison of the $U - V$ versus $V - I$ colors of resolved objects with the stellar evolutionary models of Bruzual & Charlot (2003) suggests that these sources are almost exclusively young, with likely ages of several million years (although ages derived from integrated photometry, particularly for such low-mass clusters, are subject to relatively large uncertainties). By scaling the luminosity of a 7 Myr star cluster of $10^6\,M_{\odot}$ ($M_V = -15.5$ according to Starburst99 models), we find that any young clusters that are not observed in the archival WFPC2 images would have masses of several hundred solar masses and less (i.e., $\lesssim$300–500 $M_{\odot}$). We note that this is similar to the lowest mass star cluster detected by Tremonti et al. (2001) in their study of NGC 5253 using STIS long-slit spectroscopy. Older clusters at similar luminosities could also contribute to the field and would be more massive. In §§ 5.5.3 and 5.5.4 we explore in turn the possibilities that young, low-mass clusters and older, dissolving/fading clusters contribute to our observed field regions.

5.5. *Scenarios for Understanding the Field Stellar Population*

Our main result is that the diffuse UV light in starbursts lacks the strong O star wind features observed in neighboring UV-bright star clusters. In this section we explore four possible scenarios that can explain this result:

1. Star formation occurs in both clusters and the field, but the most massive stars in the field remain in the deeply enshrouded phase longer and thus do not contribute to the UV flux.
2. Star formation occurs in both the field and clusters, but there is little or no high-mass star formation occurring in the field. This hypothesis requires that stars formed in clusters and the field have different IMFs.
3. Star formation occurs primarily in clusters, and what we are calling the field is composed of young but lower mass clusters (the low-mass end of the power-law cluster mass function), which do not form O stars.
4. Star formation occurs primarily in clusters, and as clusters age they dissolve, releasing their remaining stars into the field.

In §§ 5.5.1–5.5.4 we discuss each scenario in turn, including general implications for field formation.

5.5.1. *Are Deeply Enshrouded O Stars Hiding in the Field?*

One scenario that could explain the observed difference in massive star signatures between clusters and the field is the possibility that star formation occurs in both environments but that field O stars remain obscured (at UV wavelengths) on timescales comparable to their lifetimes and thus longer than similar stars in clusters. There are two mechanisms that influence when a massive star becomes visible at optical/UV wavelengths: (1) radiation and winds from massive stars blow out the parent molecular cloud, and (2) OB associations tend to drift away from their parent clouds, since stars and gas experience different rates of friction and thus have different velocities. In order to reproduce both the wind features and continuum slopes observed in clusters and field spectra, individual O stars formed in the field can neither blow off their natal material nor drift away from their parent cloud on timescales of $\sim$6–7 Myr; otherwise, their signature would be observed in our field spectra. This restriction would not apply to O stars formed in clusters. The typical travel time, although quite uncertain, has been given as 1–3 Myr (de Jong & Brink 1986; Leisawitz & Hauser 1988).

The problem with this scenario is that it requires fine-tuning of both drift and blowout timescales for field O stars, which must in turn be longer than those for similar stars formed in clusters. Therefore, we conclude that it is unlikely that deeply embedded, individual O stars are forming in the field regions of these starbursts, and we have just missed them because little UV flux can escape.

5.5.2. *Constraints on Field IMF*

If star formation is occurring in both field and clusters, the lack of massive stars observed in the field could arise if the IMF differs from that in clusters. We found in § 5.2.2 that instantaneous burst Starburst99 models older than 6–8 Myr produce reasonably good fits to the field spectra. However, these are unlikely to be realistic representations of spatially extended field regions. Because these field regions cover a minimum linear distance of $\sim$100 pc, it is unlikely that all the stars formed at the same time. Here we compare continuous star formation models with the extracted field spectra and discuss implications. These models take $\sim$10 Myr to equilibrate, after which the FUV spectrum changes very little as a function of age. Therefore, we fix the age at 50 Myr and assume a standard Salpeter IMF (slope $\alpha = -2.35$) and lower mass cutoff $M_{\rm low} = 1\ M_{\odot}$ (the results of our UV spectroscopy are rather insensitive to the lower mass cutoff to

TABLE 7
Best-Fitting Field Models

Galaxy	M_{up}[a]	α[b]
He 2-10	100	−2.35
Mrk 33	100	−2.35
NGC 1741	50	−3.0 to −3.5
NGC 3125	40	−3.0
NGC 3310	40	−3.0 to −3.5
NGC 4214	30	−3.5
NGC 4449	50	−3.0
NGC 4670	100	−2.35 to −3.0
NGC 5253	50	−3.0
NGC 5996	100	−3.0 to −3.5
NGC 7552	100	−2.35 to −3.0
Tol 1924−416	50	−3.0 to −3.5

[a] Best fit when field spectra are compared with continuous formation Starburst99 models that have Salpeter IMF, $M_{low} = 1\ M_\odot$, and a variable upper mass cutoff.

[b] Best fit to the IMF slope, α, in continuous formation Starburst99 model.

the IMF). There are two possible scenarios that can explain the lack of massive stars observed in field regions; both assume implicitly that star formation is occurring in situ in the field. In the first set of models, we fix the age of the continuous star formation episode at 50 Myr, assume a Salpeter IMF, and determine whether our field spectra are consistent with an upper mass cutoff that differs from that for clusters. The second set of continuous star formation models fits for the best IMF slope, with an upper mass cutoff of 100 $M_\odot$.

For the first set of models where we fit for the upper stellar mass cutoff, we have recorded the best fit in the second column of Table 7. Qualitatively, the lack of massive stars that is expressed by older ages when comparing with instantaneous burst models translates to upper mass cutoffs lower than 100 $M_\odot$. The effect of varying the upper mass cutoff is shown in the middle panels of Figure 3. Clearly, as the upper mass cutoff is lowered from 100 $M_\odot$, the signature of massive stars, particularly the P Cygni profiles for N v λ1240, Si iv λ1400, and C iv λ1550, disappears. In order to reproduce the observed field spectra, the upper stellar mass cutoff in these models has to be lowered from the 100 $M_\odot$ used in the instantaneous burst models, which provides a good fit for the clusters. For the field spectra in most target galaxies, particularly in the nearest galaxies and those distant ones that also do not show the signature of massive star wind lines, the preferred upper mass cutoff is 30–50 $M_\odot$.

A second possibility is that the IMF of stars formed in the field is steeper than for those forming in clusters. For example, Massey et al. (1995) find field stars as massive as those formed in clusters and associations in the Magellanic Clouds, even after ensuring that runaway stars are excluded. We tested this possibility by comparing a continuous Starburst99 model fixed at an age of 50 Myr, with lower and upper mass cutoffs of 1 and 100 $M_\odot$, respectively, and allowed the slope of the IMF, α, to vary between a normal Salpeter value of −2.35 and the −5.0 found by Massey et al. (1995) for the field in portions of the Magellanic Clouds. The most important influence of the massive stars is seen in the wind lines, and so we only weighted N v λ1240, Si iv λ1400, and C iv λ1550 in our fits. In the right panels of Figure 3 note in particular the rapidly decreasing strength in the N v λ1240 line. We find in general that the preferred value of α is between −3.0 and −3.5. This is steeper than Salpeter, but not as steep as found for the Magellanic Clouds. Comparison of our extracted field regions with continuous star formation models rules out an IMF slope as steep as −4.0 for our galaxies. Due to the possibility that our extracted field regions include star clusters and hence some additional massive stars that would result in a flatter slope, our values of α represent a firm lower limit to the field IMF slope. Therefore, if star formation is occurring in situ in the field and not as a result of dissolving or aging star clusters, the field is much less likely to produce massive stars than the cluster environment.

5.5.3. *Constraints on the Contribution of a Young Cluster Population to the Field*

The ultraviolet emission from the field regions surrounding star clusters in our target starbursts, in all cases with the exception of He 2-10, lacks the strong O star wind lines of N v, Si iv, and C iv that are signatures of the most massive stars. This lack of high-mass stars is not due to undersampling field regions in nearby starbursts, as the field regions contain a considerable amount of light. If we reject that the IMF slope and upper stellar mass cutoff of field regions differ from those found in clusters, there are two remaining possibilities that can explain both the observed spectral signature of the UV field and the strength of the faint peaks in the field regions. One possibility is that the field is composed of clusters that are coeval with those observed in our slit but have lower masses. The second is that the field is made up of older/dissolving star clusters. The difference in these two scenarios is primarily one of *age*. Although galaxies almost certainly form clusters with a range in both age and mass, for simplicity we assume here that the presumed population formed coevally with the luminous clusters. These clusters would represent the lower extension of the observed power-law cluster luminosity function (see, e.g., Whitmore 2003 and references therein).

We determined in the previous section that clusters with ages of several million years and masses of several hundred solar masses would not have sufficient S/N to be classified as clusters in our spectra, even in galaxies closer than 4 Mpc. Furthermore, despite their youth, it is reasonable to expect that such low-mass clusters may be lacking in the most massive O stars yet still be able to form B stars.

There are two current arguments regarding how the upper mass portion of the stellar IMF is populated in lower mass clusters. The first suggests that the distribution of stellar masses is a random sampling of the initial stellar mass function, which naturally would result in the formation of very few massive O stars in lower mass clusters. For example, a recent study by Oey et al. (2004) of the number of OB stars per cluster or association (N_*) in the Small Magellanic Cloud concludes that the distribution of N_* is consistent with these being the most massive stars in groups of lower mass stars. The second argument (e.g., Weidner & Kroupa 2004) suggests that there is a fundamental upper stellar mass limit that depends on the total mass of a cluster. From their Figure 4, a cluster at the detection limit of our study would have an upper *stellar* mass limit of ∼10 $M_\odot$. We performed a simple experiment to investigate whether stars with masses $\gtrsim$20 $M_\odot$ (∼O stars) are likely to form in clusters with masses of a few times $10^2\ M_\odot$. We randomly drew stars with masses between 0.1 and 100 $M_\odot$, from a distribution having a Salpeter slope (−2.35). Out of 1000 such simulated clusters, roughly 200–300 had at least one star more massive than 20 $M_\odot$. Therefore, if young, lower mass clusters dominate the diffuse UV light, our limits imply that there must be a sliding upper stellar mass limit, which is related to the total mass of the cluster, as suggested by Weidner & Kroupa (2004).

5.5.4. *Constraints on the Timescale of Dissolving Cluster Contribution to the Field*

Because the field regions of starbursts contain less massive stars than the clusters, a fourth possibility is that the main difference between the cluster and field stellar populations is truly one of age. The field could be composed of stars that originally formed in clusters but dissolved and released their remaining stars to the field. If the field is the product of dissolving star clusters, then we can place constraints on the timescales on which clusters in these starbursts must disintegrate. Based on the youngest and dominant ages of the field compiled in Table 4, when compared with those for star clusters, we suggest that clusters that contribute to the field need to be destroyed on very rapid timescales, of order 7–10 Myr.

The evolution of cluster systems in general includes a number of disruptive processes, such as mass loss from stellar evolution and stellar evaporation due to external gravitational shocks and internal two-body relaxation (e.g., Fall & Zhang 2001). However, these mechanisms occur over relatively long timescales ($\gtrsim 10^8$ yr) when compared with the 7–10 Myr estimated above. A recent study of the age distribution of star clusters in the Antennae galaxies suggests a very rapid decline. Fall (2004) and Fall et al. (2005) find that the number of clusters as a function of age falls by a factor of $\sim$10 by the time the cluster population has reached an age of 10 Myr. This rapid decline is seen for different mass ranges above $3 \times 10^4\ M_\odot$. Number counts of embedded clusters in the solar neighborhood with masses lower by factors of $10–10^2$ also show a similar steep decline (Lada & Lada 2003). Fall et al. (2005) suggest that this short disruption timescale indicates that the majority of (but not all) star clusters in the Antennae end up gravitationally unbound, even if the cloud from which they initially formed was initially bound. The ionizing radiation, stellar winds, and supernova explosions from massive stars could easily remove a significant fraction of the ISM from a protocluster, leaving the stars within it gravitationally unbound and freely expanding. If this is the case, such clusters would become very difficult to detect after $\sim$10 Myr. The very short timescales for cluster dissolution inferred from our data in local starburst galaxies, if dissolving clusters are responsible for the diffuse UV field emission, are consistent with the timescales of cluster disruption predicted by the free expansion model. The advantage of using UV spectroscopy, as we have done here, is the ability to track the presence of the most massive stars and directly translate these into age differences between clusters and the field.

5.6. *High-S/N Field Template*

The differences observed in the field and cluster spectra of our galaxy sample have potentially important implications for the rest-UV observations of galaxies at high redshift. Because of their small angular extent, entire galaxies are observed at high redshift, while the best local counterparts are studied in a more piecemeal way. Because the diffuse UV light from starbursts typically dominates the output from stellar clusters, it is very important to include this as an ingredient in spectral synthesis of galaxies at high redshift (although Steidel et al. [1996] show that a comparison of $z \sim 3$ Lyman break galaxy spectra with those of individual local clusters also gives reasonable fits).

We have combined the extracted field spectra for five metal-poor galaxies (Mrk 33, NGC 4214, NGC 4449, NGC 4670, and NGC 5253) that do not show the signature of massive stars, in order to make a high-S/N template of a low-metallicity "field" spectrum[9] (Fig. 6). Typical abundances for the galaxies are $\sim\frac{1}{3}-\frac{1}{5}$ solar, which is a good match to abundances measured for high-redshift galaxies (Pettini et al. 2000). This has a characteristic spectrum that is "older" than individual clusters (i.e., lacking the signature of massive stars) and is well represented by continuous star formation models.

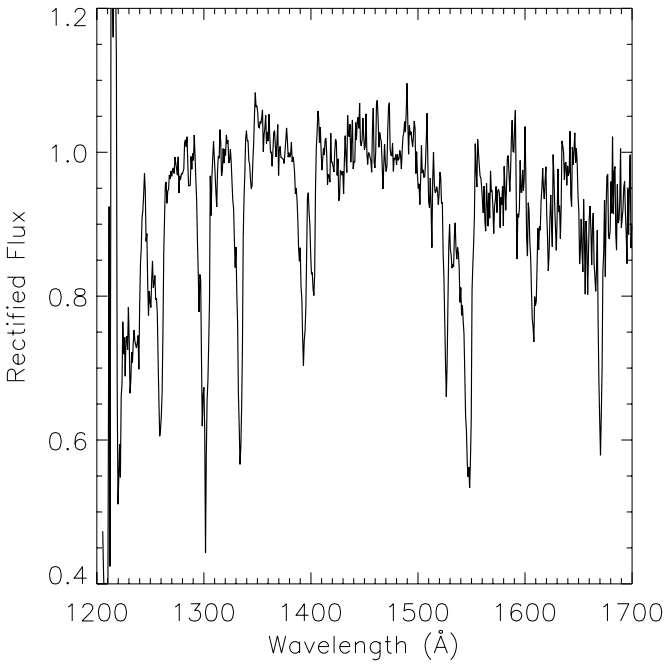


FIG. 6.—Rectified spectrum of the unweighted sum of field regions for six low-metallicity galaxies that have B star–dominated field spectra (Mrk 33, NGC 4214, NGC 4449, NGC 4670, NGC 5253, and NGC 1741).

6. SUMMARY AND CONCLUSIONS

We have used STIS long-slit FUV spectra of 12 local starburst galaxies to study the stellar content of the diffuse, UV-luminous field regions found between prominent star clusters. The extracted spectra are compared with Starburst99 stellar evolutionary synthesis models. He 2-10 is unique to our study, in that it contains the signature of massive O stars in the field regions. The composite field spectrum is very similar to that for four coeval clusters in our slit. We estimate that 40% of the light in the FUV comes from observed compact star clusters, providing a firm lower limit to the amount of UV light originating in clusters in this starburst.

With the exception of He 2-10, the clusters and field regions in the other 11 target galaxies exhibit pronounced differences. Most of the UV-bright clusters are quite young ($\lesssim$6 Myr) and show the strong P Cygni profiles found in O stars. The neighboring field regions, however, clearly lack these wind features. In particular, the nearest galaxies (NGC 4214, NGC 4449, and NGC 5253), as well as a number of more distant ones, have B star–dominated field spectra.

We include an analysis of *UVI* WFPC2 imaging for these three closest galaxies, in order to better understand the stellar populations that contribute to the field. Photometry of observed sources in all three galaxies reveals populations of blue resolved and unresolved sources. The colors and luminosities of resolved objects are indistinguishable from those of unresolved

[9] The template field spectra are available from the Starburst99 Web site: http://www.stsci.edu/science/starburst.

sources. This suggests the presence of low-mass, resolved star clusters, as well as a dispersed population of blue stars. Because we see no evidence for the presence of O stars in the field regions of these galaxies based on our (limited coverage) STIS spectroscopy, we suggest that these are a dispersed population of B stars.

The spatial profiles along the slit show that the field regions are not smooth, but rather contain numerous faint peaks and valleys. An analysis of the faint peaks in the field regions of our STIS spectra suggests that these arise from discrete stellar populations. Roughly 30%–60% of these peaks are resolved. Our calculations show, however, that the STIS spectra are just sufficient to detect the continua from unreddened, individual early B supergiants in the field. Therefore, while the population of dispersed B stars discovered in the archival WFPC2 images probably does contribute to the field spectra, they are probably not responsible for all of the faint peaks we observe. We conclude that a significant fraction of these faint peaks are likely small groups or clusters of stars, regardless of whether they are resolved or not.

We explore four possible scenarios to explain our observation that the field contains lower mass stars than neighboring clusters:

1. If star formation occurs in situ in both clusters and the field, and O stars formed in the field stay in the enshrouded phase longer than their counterparts in clusters, then these stars would not contribute much to the field UV flux. This scenario would require a "fine-tuning" of both secular drift velocities and blowout timescales for field O stars. Therefore, we believe that it is unlikely that deeply embedded, individual O stars are forming in the field regions of starbursts.

2. If star formation occurs in both field and cluster environments, the field IMF must differ from that found in clusters. If the field IMF has a normal Salpeter slope, our data are consistent with an upper mass cutoff of 30–50 $M_{\odot}$. Alternatively, the field IMF slope, α, is steeper than Salpeter, with best-fit values of -3.0 to -3.5.

3. If star formation is occurring primarily in clusters and associations, then the field could be composed of young, coeval but lower mass clusters. Our photometry and spectroscopy both imply limits of several hundred solar masses for groups or clusters of young stars that could be hiding in our field spectra. This limit is consistent with a lack of O stars only if there is an upper stellar mass limit that scales with the total cluster mass. So, effectively, this is similar to scenario 2.

4. If star formation occurs primarily in clusters, but these clusters dissolve to create the observed field, our analysis suggests that clusters must dissolve on very rapid timescales, of the order of 7–10 Myr. This is consistent with a recently presented scenario where most star clusters, almost independent of total mass, freely expand and rapidly disrupt.

We thank the anonymous referee, whose suggestions improved the presentation of this paper. We are grateful for support from NASA through grant GO-09036.01-A from the Space Telescope Science Institute, which is operated by AURA, Inc., for NASA under contract NAS5-26555. C. A. T. acknowledges support from NASA grant NAG 58426 and NSF grant AST 03-07386, and G. R. M. acknowledges support from NASA grant NAG5-13083.

REFERENCES

Annibali, F., Greggio, L., Tosi, M., Aloisi, A., & Leitherer, C. 2003, AJ, 126, 2752
Barth, A. J., Ho, L. C., Filippenko, A. V., & Sargent, W. L. 1995, AJ, 110, 1009
Bertin, E., & Arnouts, S. 1996, A&AS, 117, 393
Biretta, J. A., et al. 2000, WFPC2 Instrument Handbook, Version 5.0 (Baltimore: STScI)
Boeker, T., van der Marel, R. P., Mazzuca, L., Rix, H.-W., Rudnick, G., Ho, L. C., & Shields, J. C. 2001, AJ, 121, 1473
Bruzual, G., & Charlot, S. 2003, MNRAS, 344, 1000
Calzetti, D., Meurer, G. R., Bohlin, R. C., Garnett, D. R., Kinney, A. L., Leitherer, C., & Storchi-Bergmann, T. 1997, AJ, 114, 1834
Chandar, R., Leitherer, C., & Tremonti, C. A. 2004, ApJ, 604, 153
Chandar, R., Leitherer, C., Tremonti, C. A., & Calzetti, D. 2003, ApJ, 586, 939
Cheng, K.-P., et al. 1992, ApJ, 395, L29
Davidge, T. J. 1989, PASP, 101, 494
de Jong, T., & Brink, K. 1986, in Star Formation in Galaxies, ed. C. J. Lonsdale Persson (NASA CP-2466; Washington: NASA), 323
de Mello, D. F., Leitherer, C., & Heckman, T. M. 2000, ApJ, 530, 251
Dolphin, A. 2000, PASP, 112, 1397
Fagotto, F., Bressan, A., Bertelli, G., & Chiosi, C. 1994a, A&AS, 104, 365
———. 1994b, A&AS, 105, 29
Fall, S. M. 2004, in ASP Conf. Ser. 322, Formation and Evolution of Massive Young Star Clusters, ed. H. J. G. L. M. Lamers, A. Nota, & L. J. Smith (San Francisco: ASP), 399
Fall, S. M., Chandar, R., & Whitmore, B. C. 2005, ApJ, submitted
Fall, S. M., & Zhang, Q. 2001, ApJ, 561, 751
Fitzpatrick, E. L. 1999, PASP, 111, 63
Greggio, L., Tosi, M., Clampin, M., de Marchi, G., Leitherer, C., Nota, A., & Sirianni, M. 1998, ApJ, 504, 725
Guseva, N., Izotov, Y. I., & Thuan, T. X. 2000, ApJ, 531, 776
Haas, M., Lemke, D., Stickel, M., Hippelein, H., Kunkel, M., Herbstmeier, U., & Mattila, K. 1998, A&A, 338, L33
Harris, J., Calzetti, D., Gallagher, J. S., III, Conselice, C. J., & Smith, D. A. 2001, AJ, 122, 3046
Heckman, T. M., Robert, C., Leitherer, C., Garnett, D. R., & van der Rydt, R. 1998, ApJ, 503, 646
Hippelein, H., Haas, M., Tuffs, R. J., Lemke, D., Stickel, M., Klaas, U., & Volk, H. J. 2003, A&A, 407, 137
Holtzman, J. A., Burrows, C. J., Casertano, S., Hester, J. J., Trauger, J. T., Watson, A. M., & Worthey, G. 1995, PASP, 107, 1065
Humphreys, R. M. 1978, ApJS, 38, 309
Hunter, D. A. 1999, in IAU Symp. 193, Wolf-Rayet Phenomena in Massive Stars and Starburst Galaxies, ed. K. A. van der Hucht, G. Koenigsberger, & P. R. J. Eenens (San Francisco: ASP), 418
Izotov, Y. I., & Thuan, T. X. 1999, ApJ, 511, 639
Kobulnicky, H. A., Kennicutt, R. C., Jr., & Pizagno, J. L. 1999, ApJ, 514, 544
Kurucz, R. L. 1993, CD-ROM 13, ATLAS 9 Stellar Atmosphere Programs and 2 km/s Grid (Cambridge: SAO)
Lada, C. J., & Lada, E. A. 2003, ARA&A, 41, 57
Lamers, H. J. G. L. M., Panagia, N., Scuderi, S., Romaniello, M., Spaans, M., de Wit, W. J., & Kirshner, R. 2002, ApJ, 566, 818
Larsen, S. S. 1999, A&AS, 139, 393
Larsen, S. S., & Brodie, J. P. 2000, AJ, 120, 2938
Leisawitz, D., & Hauser, M. G. 1988, ApJ, 332, 954
Leitherer, C. 1998, in ASP Conf. Ser. 142, The Stellar Initial Mass Function, ed. G. Gilmore & D. Howell (San Francisco: ASP), 61
Leitherer, C., et al. 1999, ApJS, 123, 3
Maiz-Apellaniz, J., Walborn, N. R., Galue, H. A., & Wei, L. H. 2004, ApJS, 151, 103
Maoz, D., Barth, A. J., Sternberg, A., Filippenko, A. V., Ho, L. C., Macchetto, F. D., Rix, H.-W., & Schneider, D. P. 1996, AJ, 111, 2248
Massey, P., Lang, C. C., Degioia-Eastwood, K., & Garmany, C. D. 1995, ApJ, 438, 188
Massey, P., & Olsen, K. A. G. 2003, AJ, 126, 2867
Meurer, G. R., Heckman, T. M., Leitherer, C., Kinney, A., Robert, C., & Garnett, D. R. 1995, AJ, 110, 2665
Meynet, G., Maeder, A., Schaller, G., Schaerer, D., & Charbonnel, C. 1994, A&AS, 103, 97
Misiriotis, A., Popescu, C. C., Tuffs, R. J., & Kylafis, N. D. 2001, A&A, 372, 775
Oey, M. S., King, N. L., & Parker, J. W. 2004, AJ, 127, 1632
Pastoriza, M. G., Dottori, H. A., Terlevich, E., Terlevich, R., & Diaz, A. I. 1993, MNRAS, 260, 177
Pettini, M., Steidel, C. C., Adelberger, K. L., Dickinson, M., & Giavalisco, M. 2000, ApJ, 528, 96
Popescu, C. C., Misiriotis, A., Kylafis, N. D., Tuffs, R. J., & Fischera, J. 2000, A&A, 362, 138

Popescu, C. C., et al. 2005, ApJ, 619, L75
Salpeter, E. E. 1955, ApJ, 121, 161
Schlegel, D. J., Finkbeiner, D. P., & Davis, M. 1998, ApJ, 500, 525
Steidel, C. C., Giavalisco, M., Pettini, M., Dickinson, M., & Adelberger, K. L. 1996, ApJ, 462, L17
Stetson, P. B. 1987, PASP, 99, 191
Thilker, D. A., et al. 2005a, ApJ, 619, L67
———. 2005b, ApJ, 619, L79
Tosi, M., Sabbi, E., Bellazzini, M., Aloisi, A., Greggio, L., Leitherer, C., & Montegriffo, P. 2001, AJ, 122, 1271
Tremonti, C. A., Calzetti, D., Leitherer, C., & Heckman, T. M. 2001, ApJ, 555, 322
van den Bergh, S. 2004, AJ, 128, 1880
Weidner, C., & Kroupa, P. 2004, MNRAS, 348, 187
Whitmore, B. C. 2003, in A Decade of *Hubble Space Telescope* Science, ed. M. Livio, K. Noll, & M. Stiavelli (Cambridge: Cambridge Univ. Press), 153